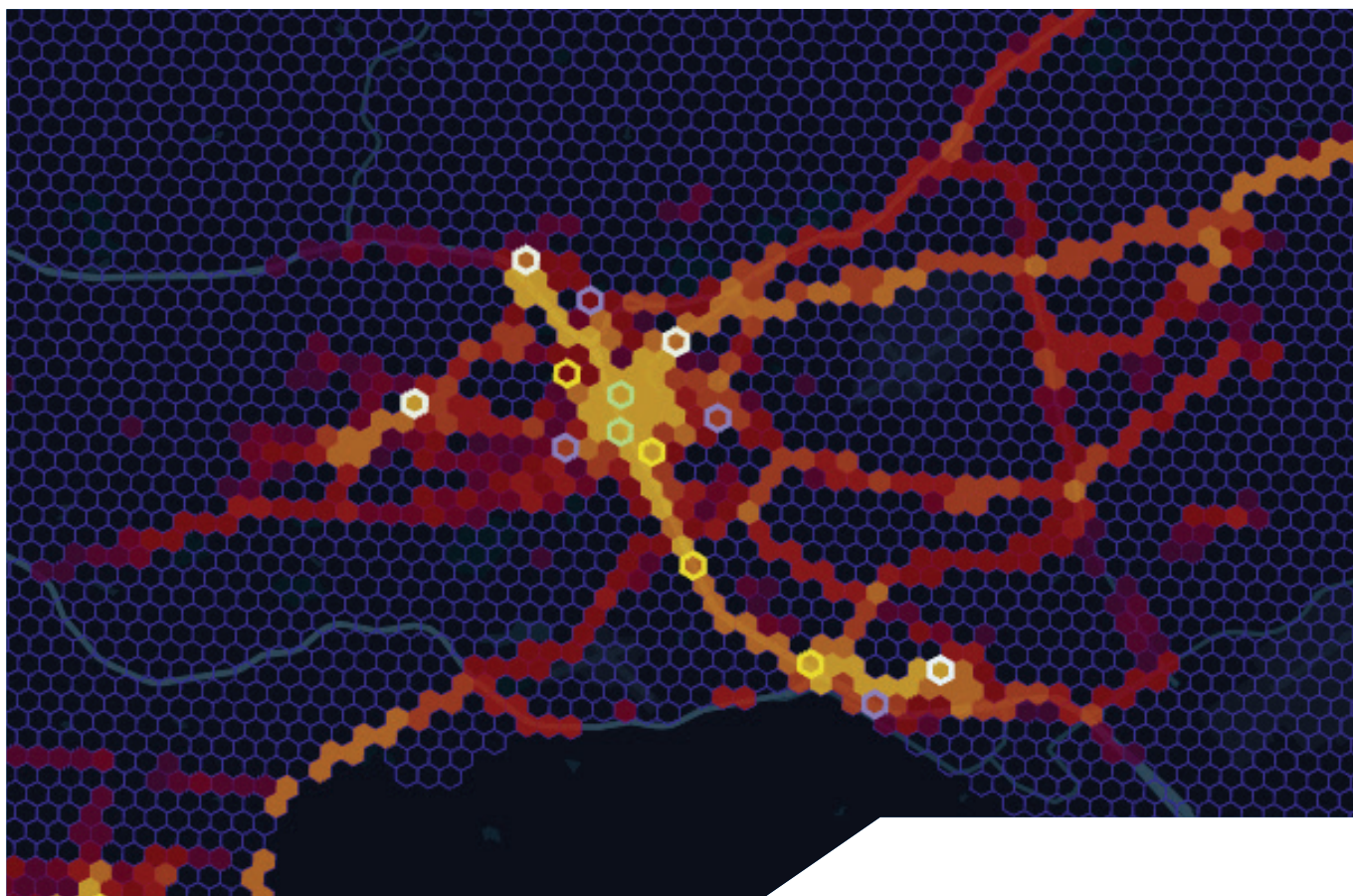


ChargeUp! Data Swap!

Using data from battery swapping e-motorcycles
in Nairobi to assess impacts and plan infrastructure



Authors

Cameron Sheehan
Professor Tim Green

About ChargeUp!

The ChargeUp! Project is funded by P4G (Partnering for Green Growth and the Global Goals 2030) to test the commercial viability of a Battery as a Service (BaaS) model by establishing a network of charging stations in Nairobi, Kenya, which will charge a flat battery swap fee for electric two- and three-wheelers. The project partners include Energy 4 Impact (E4I) as the project coordinator, Strathmore University, and Imperial College London as the academic partners, while ARC Ride and Fika Mobility are the commercial partners.

In this partnership, electric bike drivers can conveniently swap out their batteries quickly and affordably, reducing operational costs and concerns about the battery not lasting long enough to complete their activities. This model will enable an inclusive ecosystem that creates long-term green jobs for charging station mechanics and electric vehicle (EV) drivers. Expanded battery swapping infrastructure can help businesses and start-ups join the E-mobility transition. During the partnership funding period, ChargeUp! plans to establish a network of 45 operational battery charging and swapping stations in Nairobi and complete a baseline assessment for the commercial viability of a BaaS model. Ultimately, the partnership aims to develop an openly accessible and replicable master plan for e-bike adoption by cities across Africa. For more information visit: www.imperial.ac.uk/energy-futures-lab/research-projects/chargeup/

Energy Futures Lab is one of seven Global Institutes at Imperial College London. The institute was established to address global energy challenges by identifying and leading new opportunities to serve industry, government and society at large through high quality research, evidence and advocacy for positive change. The institute aims to promote energy innovation and advance systemic solutions for a sustainable energy future by bringing together the science, engineering and policy expertise at Imperial and fostering collaboration with a wide variety of external partners. www.imperial.ac.uk/energy-futures-lab

Suggested citation: Sheehan, C. and Green, T.C. (2023) *ChargeUp! Data Swap! Using data from battery swapping e-motorcycles in Nairobi to assess impacts and plan infrastructure*. Imperial College London.



Contents

About ChargeUp!	2	Results	13
Executive Summary	4	E-motorcycle trip analysis	13
Introduction	5	Battery swap demand analysis	14
Background	5	Battery charging energy	16
Aims and scope	6	Existing charging energy profiles	16
Structure of report	6	Co-ordinated charging scenario for BSSs	17
Methodology	7	Swap battery charging emissions analysis	18
Operational battery swap system data	7	Swap battery charging electricity tariff costs	21
Battery swap cabinet data	7	Optimal number of swap stations and batteries	23
Battery management system data	7	Optimal locations of swap stations based on vehicle trip data	25
Battery location data	7		
Existing battery swap cabinet location data	7		
E-motorcycle trip analysis	8	Conclusions	30
Battery swap demand analysis	8	Key findings	30
Average swaps per user per day	8	Further work	31
Battery swap probability and SOC distributions	8	References	32
Battery charging energy consumption distributions	8	Appendix A – Additional Methodology Details	34
Swap battery charging emissions analysis	9	Calculation of half-hourly emissions factors for the Kenyan grid	34
Calculation of half-hourly emissions factors for the Kenyan grid	9	Swap battery charging electricity tariff scenarios	36
Estimation of swap battery charging related emissions	10	Optimal locations of swap stations based on vehicle trip data	38
Swap battery charging electricity tariff costs	10		
Optimal number of swap stations and batteries	11		
Optimal locations of swap stations based on vehicle trip data	12		

Executive Summary

The dearth of available data on e-motorcycle usage in African cities is a significant challenge in impact studies of e-motorcycle deployment. The ChargeUp! project aimed to fill this research gap using operational data from e-motorcycles and battery swap stations in Nairobi to perform modelling and analysis to determine several key outputs. This project included the analysis of: e-motorcycle trips; battery swapping demand; battery charging energy consumption; swap battery charging related emissions for a high renewables and high fossil energy mix scenarios; charging related electricity costs for different tariff scenarios; the effect of a co-ordinated charging scenario on emissions and tariffs; optimal battery ratios and required numbers of swap stations; and a methodology to determine optimal regions for battery swap stations based on trip data.

The analysis showed that most trips by e-motorcycles are relatively short in distance, with an average trip length of 4.5 km, and an average speed of 20.1 km/h. The peak period for trips is between 17:00 and 18:00, coinciding with the evening commute. The riders seem less likely to swap out their batteries during the busiest trip periods, and when riders do swap out during the peak period, they appear to do so only when the battery state of charge (SOC) is close to reaching zero. This contrasts with swapping behaviour in the mornings, where riders appear to swap out their battery before their shift begins regardless of the battery state of charge, probably so that they can start their day with a fully charged battery. Batteries in the dataset were found to be charged at either battery swapping stations (BSSs) or away from BSSs (possibly at home or other locations using a private charger). The charging profiles for these two destination types were found to be different, especially in the evenings, where charging events away from BSSs appeared to make use of overnight charging.

Compared to Internal Combustion Engine (ICE) motorcycles, the e-motorcycles' emissions factors (EF) for all scenarios were estimated to be substantially lower, with decreases in the range of -87.8 % (E2W High Fossil Scenario) to -94.3 % (E2W High Renewables Scenario). For the High Fossil Scenario, the emissions factor was decreased by 22.7 % by implementing charging co-ordination, which shows the benefit that charging co-ordination could have on days with higher fossil-based energy in the mix. A potential E-mobility Time-of-Use (TOU) Tariff Scenario was shown to provide an increase in electricity cost savings when a co-ordinated charging strategy was implemented to shift charging away from the evening peak load. This reduction in total electricity costs could act as an incentive for BSS operators to attempt to co-ordinate their charging if the TOU tariff was in place. The results show that the proposed E-mobility Tariff Scenario provides savings of 16.4 % compared to the Domestic Tariff Scenario. If an E-mobility TOU Tariff was implemented, and the BSSs were able to co-ordinate their charging, this would lead to almost double the savings at 32.4 % as compared to the domestic tariff.

For swap stations with the specifications present for this study, the optimal battery ratio was found to be 1.66 batteries per e-motorcycle. This would mean approximately 6 BSSs for every 100 e-motorcycles if every BSS contained 11 batteries in storage. Lastly, the BSS location optimisation model can be used to determine optimal regions for BSS sites in a multi-stage deployment strategy that is informed by trip location data. Optimisation parameters can be adjusted for each deployment stage to allow different spacing and coverage constraints for each solution. The various Python data analysis models, including the BSS location optimisation model, will be released openly as part of the project.

This study was part of the ChargeUp! Project, funded by P4G (Partnering for Green Growth and the Global Goals 2030) to test the commercial viability of a Battery as a Service (BaaS) model by establishing a network of charging stations in Nairobi, Kenya.

Introduction

Background

Kenya has over 25 new e-mobility companies that are aiming to electrify vehicles across all major types [1]. Motorcycles have been identified as a key entry market for vehicle electrification considering their low charging requirements, high fleet turnover, and lifetime cost competitiveness [2]. There are estimated to be over 300 electric motorcycles (e-motorcycles) already operating in the region [1], with more being deployed every month. These motorcycles are primarily used for commercial taxi (boda-boda) and delivery services.

The two prevalent methods being used to provide energy to these vehicles are conventional charging and battery swapping. Conventional charging requires the user to plug in their battery and wait for it to charge for some time (around 2 hours but depending on the power of the charger) before they can use it again. In contrast, battery swapping allows the user to swap out their discharged battery for a fully charged one in a relatively short time (normally less than 5 minutes) at a battery swapping station (BSS), where additional batteries are kept and charged [3].

There is a general lack of data and research into how this transition to e-motorcycles may occur in Kenya and other African countries, and more specifically, what infrastructure may be needed to charge these vehicles' batteries. A recent paper on energy and transport in Africa and South Asia [4] identified key knowledge gaps that lie at the intersection between mobility and power systems. A 2019 review of spatial localisation methodologies for electric vehicle charging infrastructure found that research had been conducted in most parts of the world, except for Africa [5]. The dearth of available data on e-motorcycle usage in African cities is a significant challenge in impact studies of e-motorcycle deployment. The authors' recent contributions [6], [7] aimed to address this challenge with the use of synthetic data and the development of a novel simulation of e-motorcycle taxi usage, specifically tailored to represent usage patterns and the derived demand for battery swaps in the Sub-Saharan African context. That research highlighted further areas for work, especially the opportunity to analyse and use real data from e-motorcycles that are being trialled in case study locations as inputs, rather than synthetic data, to improve the simulation model and allow further research questions to be explored.

Aims and scope

The ChargeUp! project aimed to fill this research gap using operational data from e-motorcycles and battery swap stations in Nairobi, supplied by one of the commercial e-mobility partners (ARC Ride [8]), to perform modelling and analysis to determine several key outputs related to e-motorcycles and battery swap stations.

The primary objectives of the study were to use real analytics data from e-motorcycles and battery swap stations in Nairobi to:

1. Quantify the well-to-wheel carbon emissions mitigated by shifting to electric motorcycles from internal combustion engine (ICE) motorcycles in Nairobi and investigate the effect of charging time on emissions.
2. Investigate how different reduced-cost electricity tariff structures would affect the operating costs of battery swap stations in Nairobi.
3. Determine the optimal number of charging/swap stations and batteries needed per vehicle to have a cost-effective and complete Battery-as-a-Service (BaaS) ecosystem in Nairobi.
4. Determine the optimal locations for the deployment of charging/swap stations in Nairobi.

In addition to these primary objectives, additional analyses were performed to shed light on e-motorcycle trip statistics and battery swapping demand in Nairobi, based on the data received.

The scope of the study is limited to e-motorcycles and battery swap stations in Nairobi, based on the data that was received. Due to unforeseen circumstances, there were delays in the deployment of vehicles and battery swapping infrastructure during the project that led to a delay in receiving data for modelling and analysis. Therefore, this study was based on a smaller dataset than had initially been planned for the project. However, it is hoped that the analysis methodology developed here can be applied to larger datasets in future as they become available.

Structure of report

The structure of this report is as follows. First, the background and aims of the report are detailed in the Introduction section. Next, for brevity, a brief description of the methodologies used for the various analyses is provided in the Methodology section, with references to relevant appendices that contain more detailed information. The Results section that follows provides and discusses the results from each of the analyses. Finally, the conclusions and areas for further work are detailed in the Conclusion section.

Methodology

Operational battery swap system data

This analysis used various types of data from an operational battery swapping system for e-motorcycles in Nairobi between 10th December 2022 to 9th March 2023 (3 months). The data was provided as secondary data by ARC Ride [8], one of the ChargeUp! commercial partners. All data was pseudonymised by the commercial partner prior to sharing to ensure that no personal details were included in the datasets. The various datasets are detailed below.

Battery swap cabinet data

This dataset comprised of 461 data records related to the batteries swapped at each of the seven battery swap cabinets that were operating within Nairobi. The dataset fields required for the analysis were the following:

- Battery swap timestamp
- Pseudonymised ID of swap cabinet where swap occurred
- Pseudonymised ID of user
- Pseudonymised ID of incoming swap battery
- Pseudonymised ID of outgoing swap battery
- State of Charge (SOC) of incoming swap battery (%)
- State of Charge (SOC) of outgoing swap battery (%)

Battery management system data

This dataset comprised of 2,335,086 data records related to the battery management systems (BMS) of 35 swap batteries operating within Nairobi. The dataset fields required for the analysis were the following:

- Timestamp of data record
- Pseudonymised ID of swap battery
- State of Charge (SOC) of swap battery (%)

Battery location data

This dataset comprised of 680,673 data records related to the locations of 35 swap batteries operating within Nairobi. The dataset fields required for the analysis were the following:

- Timestamp of data record
- Pseudonymised ID of swap battery
- Longitudinal co-ordinate of swap battery
- Latitudinal co-ordinate of swap battery

Existing battery swap cabinet location data

This dataset comprised of 7 data records related to the locations of the battery swap cabinets that were operating within Nairobi. The dataset fields required for the analysis were the following:

- Pseudonymised ID of swap cabinet
- Location description
- Longitudinal co-ordinate of swap cabinet
- Latitudinal co-ordinate of swap cabinet

E-motorcycle trip analysis

The battery location data was used to determine various trip statistics related to the e-motorcycles that were using the batteries. First, the raw GPS co-ordinates and their timestamps were processed to detect individual trajectories (trips) for each battery using *MovingPandas* [9], a Python library developed for the analysis of movement data. The individual trajectories were split between stopping points, which were detected when the co-ordinates of the batteries remained within a circular region with a specified diameter (200 m) for a minimum length of time (5 minutes). The stop detection diameter value was chosen through trial and error to minimise the effect of any GPS location inaccuracy when the batteries were stationary from being detected as movement. The minimum stopping time was chosen to prevent short stops caused by traffic, or other reasons, from splitting the trips erroneously. For each detected trip, the start time, end time, trip duration, trip distance, and average trip speed were determined and recorded for further analysis.

Battery swap demand analysis

The following aspects of battery swapping demand at the battery swap stations were investigated.

Average swaps per user per day

The total number of swaps per unique user was calculated for each day in the dataset and then averaged to determine the average number of swaps per user per day.

Battery swap probability and SOC distributions

Using the timestamp of the battery swaps in the battery swap cabinet dataset, the probability distribution of battery swap occurring on days of the week as well as within other time periods, such as every hour or half-hour in day, was determined. Similarly, the distributions of state of charge (SOC) for incoming batteries at the swap stations for different time periods was determined.

Battery charging energy consumption distributions

No data was available for the power and energy usage at the battery swap stations; therefore, the charging energy was estimated by using the SOC values of the batteries from the BMS data. First, the change in SOC value between successive records for each battery was determined. For a positive SOC change, i.e., an increasing battery charge level, the battery was classified as charging. The increase in a battery's energy during charging (kWh) was then calculated by multiplying the positive SOC change (%) by the total energy storage capacity of the battery (2.1 kWh), assuming that the relationship between stored energy and SOC was linear and that the battery was at nominal temperature. All charging energy values calculated for each timestamp were then aggregated for various time periods, such as every hour or half-hour in the day. To calculate the charging energy provided by the grid, the efficiency of the chargers (90%) were also considered.

To determine whether a charging event occurred at a BSS, the GPS and BMS datasets were merged using the battery ID values and the closest corresponding timestamp. A maximum time difference between the timestamps of the two different datasets was limited to 30 seconds. This was to prevent BMS data from being linked to GPS co-ordinates too far from the actual location that the timestamp occurred.

Swap battery charging emissions analysis

For the calculation of charging related emissions from the Kenyan grid, investigation of how the timing of the charging affected the emissions was of interest. Therefore, time-of-use (TOU) emissions factors (EF) were required, however, none were found for Kenya’s electricity system. The methods to determine these TOU EFs for Kenya, and their use in calculating charging related emissions for the swap battery system are detailed below.

Calculation of half-hourly emissions factors for the Kenyan grid

Since no TOU EFs were found for Kenya, the authors made use of available data to determine these factors for the analysis. Further details of the methodology used are provided in Appendix A, and an overview is provided here.

Two representative day energy mix profiles [10] were used to determine TOU EF scenarios, one for a day with high renewables availability (High Renewables Scenario), and one with low renewables availability (i.e., High Fossil Scenario). The demand profiles for each scenario are shown in Figure 1 and Figure 2.

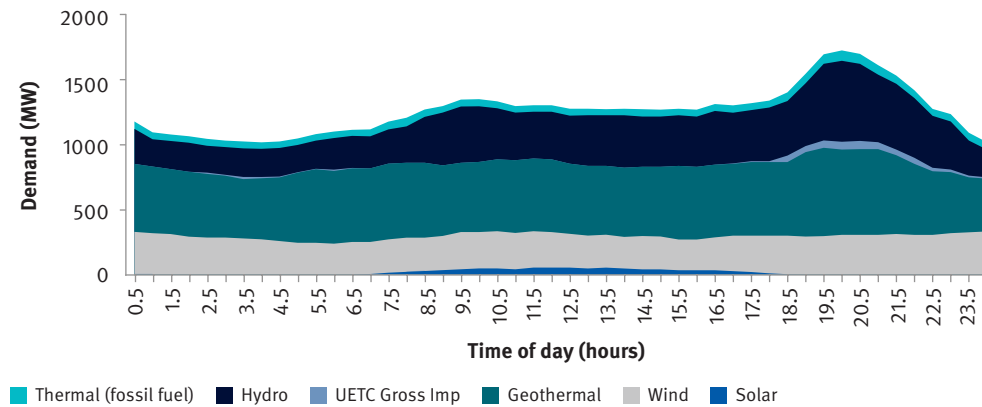


Figure 1: Kenyan day demand profile (high renewables scenario). Source: Author, using data from [10]

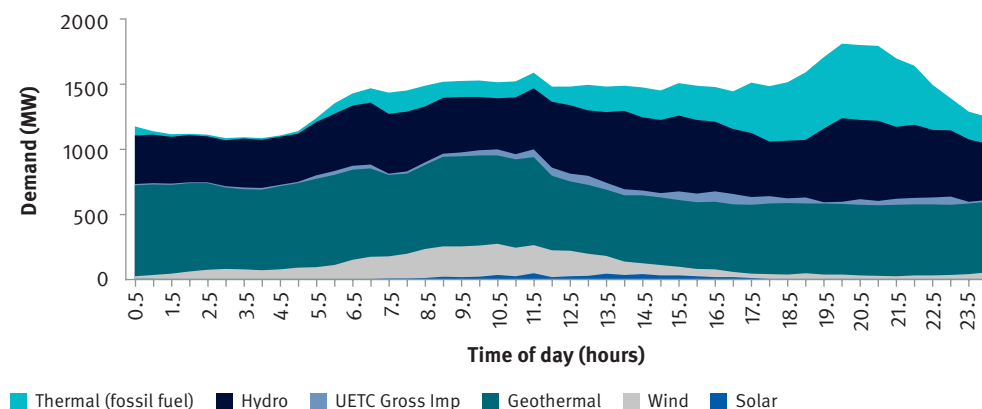


Figure 2: Kenyan day demand profile (high fossil scenario). Source: Author, using data from [10]

Based on the energy mix in each scenario, the half-hourly average emissions factors (AEFs) for each scenario were determined (kgCO_2). Note that the CO_2 equivalent emissions factors weren't available, so direct CO_2 emissions factors were used in the analysis. The resulting AEFs are shown in Figure 3.

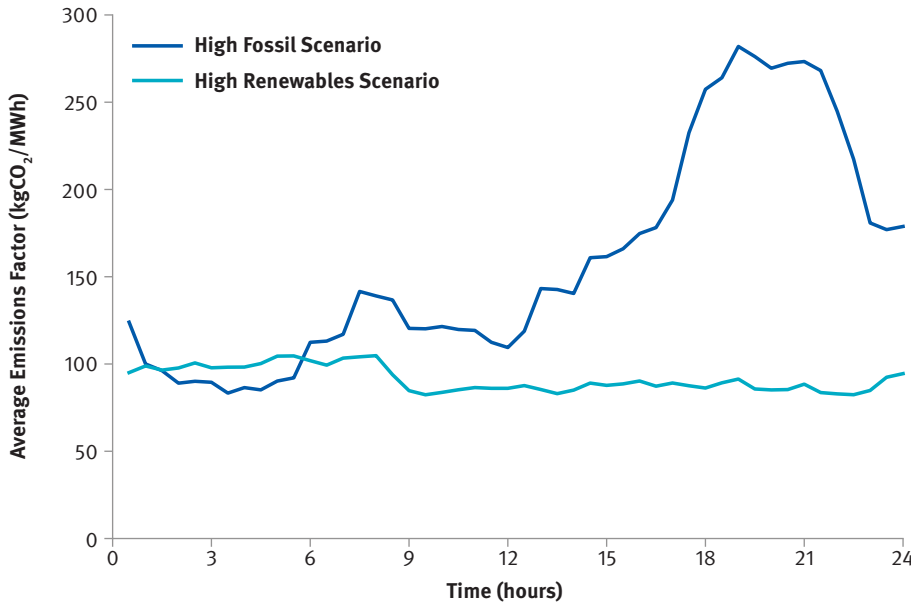


Figure 3: Average emissions factors for the high renewables scenario and high fossil scenario. Source: Author

As shown in Figure 3, the AEFs for the High Fossil Scenario are much higher during the afternoon and evening peak period when the fossil fuelled power plants are providing a higher percentage of the total energy mix. The High Renewables Scenario has a much lower AEF with less variation throughout the day.

Estimation of swap battery charging related emissions

Using the battery charging energy consumptions calculated for half-hourly periods, the associated emissions could be calculated using the half-hourly AEFs. Multiplication of the energy usage (MWh) with the AEFs (kgCO_2/MWh) results in the emissions during that period (kgCO_2).

The emissions factors of the e-motorcycles on a per distance basis (gCO_2/km) were calculated by considering the total distance travelled and total emissions from charging the batteries. The baseline emissions factor for Internal Combustion Engine (ICE) motorcycles in Kenya was assumed to be $69.1 \text{ gCO}_2/\text{km}$ as stated in a report on updated transport data in Kenya [11].

Swap battery charging electricity tariff costs

To investigate the effects of different electricity tariffs on charging costs, three different tariff scenarios were explored, as detailed in Table 1. Further details of the methodology used are provided in Appendix A.

Table 1: Tariff scenarios summary

Tariff scenario	Hours	Base tariff (KShs/kWh)	Elec. cost (KShs/kWh incl. VAT)
Scenario 1: Domestic [12]	Peak	21.50	38.69
	Off-peak	21.50	38.69
Scenario 2: E-mobility [12]	Peak	17.00	33.25
	Off-peak	17.00	33.25
Scenario 3: E-mobility TOU*	Peak	17.00	33.25
	Off-peak	8.50	22.96

*E-mobility time-of-use (TOU) tariff scenario developed by authors

The Domestic and E-mobility tariffs are based on the July 2023 tariffs in the Kenya Power and Lighting Company's (KPLC) retail tariff application to the Energy and Petroleum Regulatory Authority (EPRA) [12]. The third scenario was developed by the authors to explore the impact of providing an E-mobility time-of-use (TOU) tariff structure, where the base tariff is discounted at 50% during off-peak hours as is done with other KPLC TOU tariffs [12]. Note that the electricity costs shown in Table 1 are based on the base tariff with all surcharges and VAT included. Details of the surcharges are provided in Appendix A.

Using the battery charging energy consumptions calculated for hourly periods, the charging energy costs could be calculated using the electricity cost at each hour for each scenario.

Optimal number of swap stations and batteries

To determine the optimal number of swap stations and batteries required for a set number of e-motorcycles, a battery swapping simulation was run using a hybrid model (continuous and discrete processes) developed during previous work by the authors [6], [7]. The model was adapted for this study to allow a set number of battery swapping stations (BSSs) to be simulated at the same time, with arriving e-motorcycles being randomly allocated to join the queue at a BSS in the system. The number of BSSs was varied for a set number of e-motorcycles, and the reliability of the system was assessed. For this assessment, reliability was defined as the percentage of arriving vehicles that were served a fully charged battery within 5 minutes of arriving at the BSS. Once an optimal battery ratio (BR) has been determined for the specified system, the number of required BSSs, $N_{BSS, req}$, can be determined using Eq. (1).

$$N_{BSS, req} = \frac{N_{E2W} (BR - 1)}{N_{batt/BSS}} \quad (1)$$

Where N_{E2W} is the number of e-motorcycles and $N_{batt/BSS}$ is the number of batteries per BSS.

Optimal regions for swap stations based on vehicle trip data

To determine optimal locations of battery swap stations based on vehicle trip data, a Mixed Integer Linear Programming (MILP) optimisation model was developed and implemented in Python. The methodology was based on the work of [13], where charging station locations were optimised for urban taxi providers, by partitioning the analysis area into a set of hexagons (H). However, for the analysis detailed here, battery swap stations are optimally located instead of charging stations, and battery swapping demand was assumed to be correlated with regions that had a higher number of trips that passed through them, since battery swapping could be done within a few minutes on the way to any location. Further details on how the method from study [13] was adapted and implemented for this study are described in Appendix A.

Note that optimal regions are determined using this methodology, rather than specific sites, as this allows the planner to do more detailed site selection within a chosen optimal region as the final step, as discussed in [13]. This method seemed appropriate for this study use case, where experience during the ChargeUp! project has shown that final site selection for a BSS requires several additional considerations. These considerations may include, inter alia, the availability of local businesses to partner with, local planning regulations, parking availability, and electrical infrastructure requirements at the site. This optimisation tool could be used to assist BSS planners to determine which regions they should focus on for their detailed site selection process. It's anticipated that the BSS deployment process will be iterative in practice, with BSS operators growing their network by only a few new BSSs at a time as they deploy more vehicles. Therefore, the tool could be used in a similar iterative manner, using data from existing BSSs and vehicles to determine the next set of optimal regions to locate new BSSs.

Results

In this section, we present the results based on the analysis of the datasets described in the Methodology section. First, various results related to e-motorcycle trips are provided, followed by results from the battery swap demand analysis, emissions analysis, and tariffs analysis. Next, the optimal battery ratio is investigated for a specified swap station system scenario. Finally, the optimal location results are shown for an illustrative three stage deployment strategy for the placement of 30 new swap stations in Nairobi.

E-motorcycle trip analysis

The total distance of all detected trips came to 18,213 km, with an average trip distance of 4.48 km.

As shown in the trip distance histogram in Figure 4, the most frequent trip distance was between 1–2 km. The majority of trip distances are less than 6 km, with the 75th percentile of all trip distances being 5.5 km.

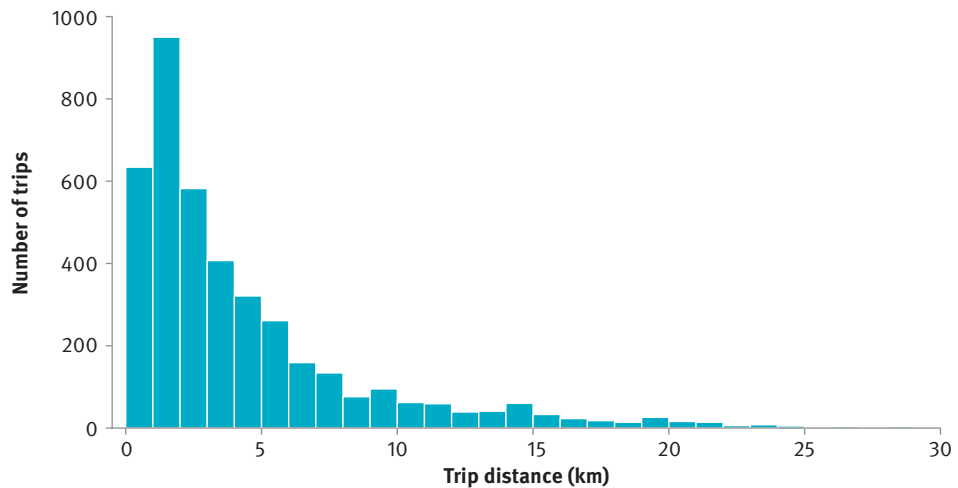


Figure 4: Histogram of trip distances

The average and median trip speed of all trips detected in this dataset were 20.1 km/h and 18.7 km/h respectively. The distribution of average trips speeds is shown in Figure 5.

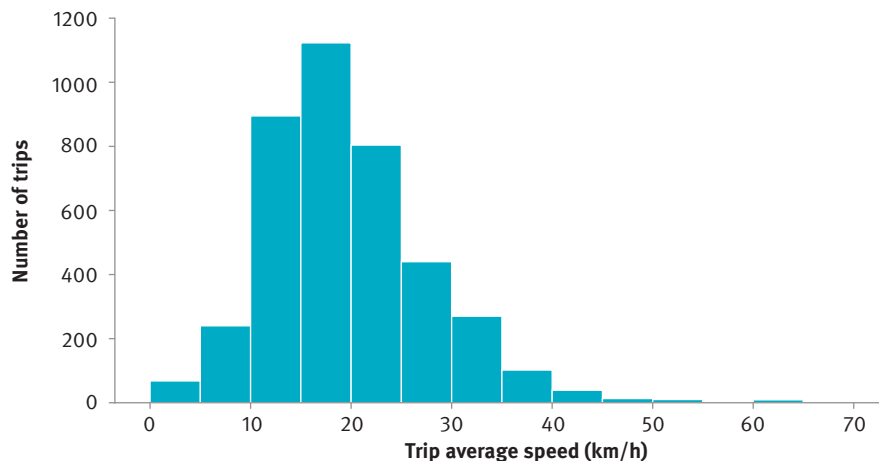


Figure 5: Histogram of average trip speeds

The distribution of trip start times is shown in Figure 6.

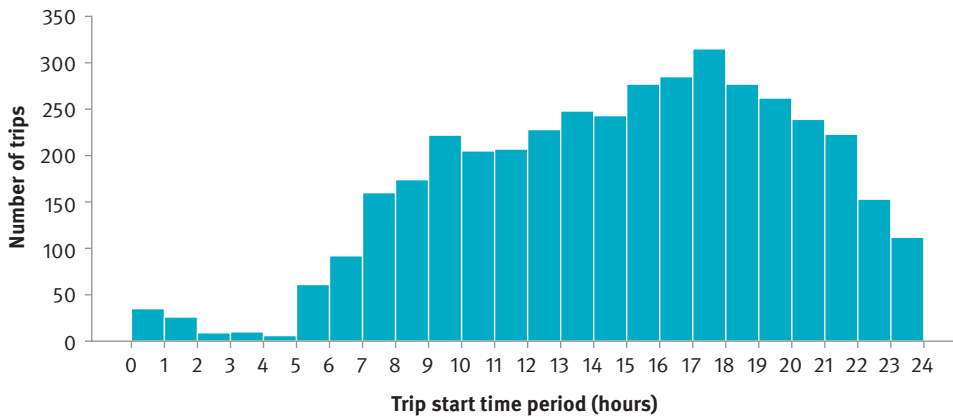


Figure 6: Histogram of trip start times

The number of trips starting in each hour steadily increase in the morning, from the period 5:00–6:00, to a peak in the evening in the period 17:00–18:00. The morning peak appears to be in the period 9:00–10:00. For e-motorcycles being used as taxis, the morning and evening peak most likely coincides with commuters getting rides to or from work. The number of trips starting in each hour then gradually decreases between 18:00 and the early hours of the next morning.

Battery swap demand analysis

The probability of battery swaps occurring at different hours in the day is shown in Figure 7.

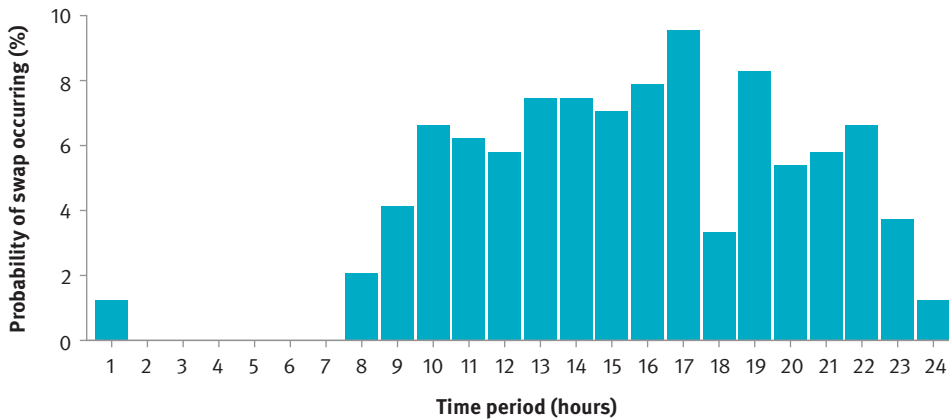


Figure 7: Battery swapping probability for each hour in day

The swap probabilities have a similar distribution to the trip start times shown in Figure 6, except that during the 18th hour in the day (17:00–18:00), the probability of swaps occurring drops substantially while the trip start times reach their peak. This may imply that during the busiest trip periods, the riders are less likely to swap out their batteries.

The distribution of state of charge (SOC) values for the arriving batteries at the battery swap stations in this dataset is shown in Figure 8.

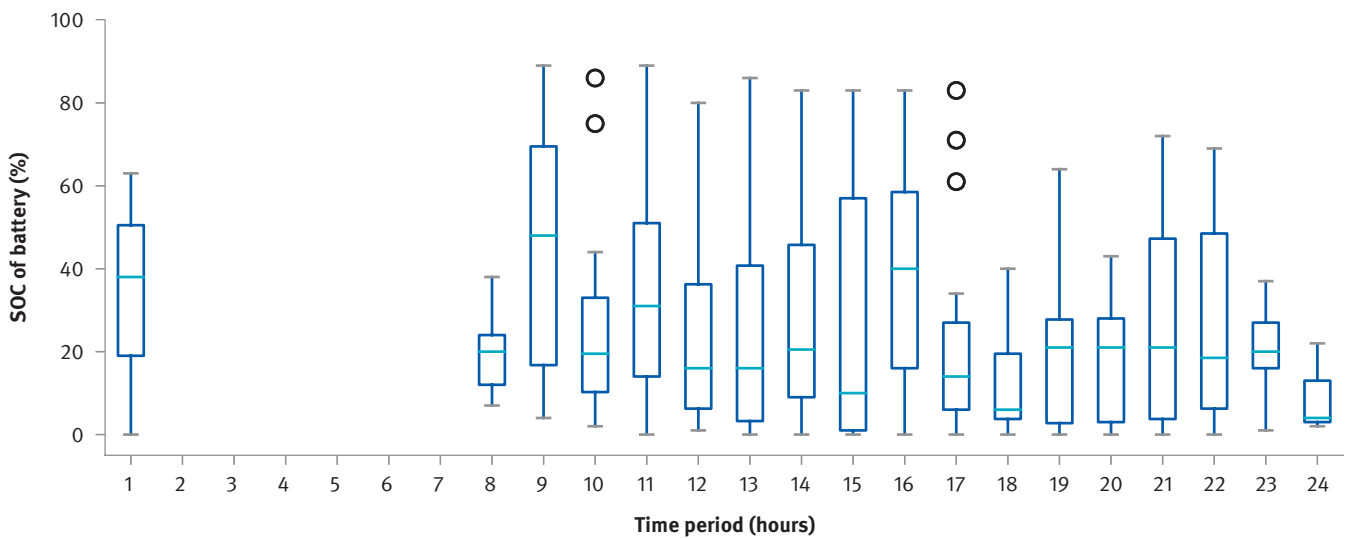


Figure 8: Boxplot of state of charge (SOC) values of batteries arriving at the swap stations

The boxplot shows that batteries swapped out in the 9th hour (8:00–9:00) arrive with a relatively wide range of SOC values, with 50% of batteries being in the range of 20 – 70% SOC, and a relatively high median SOC value of 50%. This high range of SOC values in that morning period may be due to riders preferring to swap out their battery in the morning before their shift begins, regardless of the battery state of charge, so that they can start their day with a fully charged battery. This is just a hypothesis and would need to be validated in further work, potentially by interviewing riders about their preferences around swapping times. The median SOC values at other times of the day are relatively low, mostly in the range of 10–30%, as riders decide to swap their battery before it gets too low. During the peak trip period of the 18th hour in the day (17:00–18:00), the median SOC value is very low at around 5%. This is in line with the hypothesis that riders are less likely to swap during the busiest trip periods and may only decide to swap their battery out if it is absolutely necessary. In this case, continuing with trips after the battery has reached a 5% SOC value will increase the likelihood that a rider might run their battery flat (0% SOC) during their trip, which would result in them being stranded if they didn't swap their battery. Again, this hypothesis would need to be validated in further work.

Battery charging energy

The average energy intensity of the e-motorcycles during the analysis period was calculated to be 0.045 kWh/km based on the total energy consumed (812.8 kWh) and total distance driven (18,213 km). The battery charging energy distributions are detailed below for existing charging profiles and a hypothetical co-ordinated charging scenario.

Existing charging energy profiles

The total energy for all detected charging events in the dataset were aggregated for each hour in the day, as shown in Figure 9.

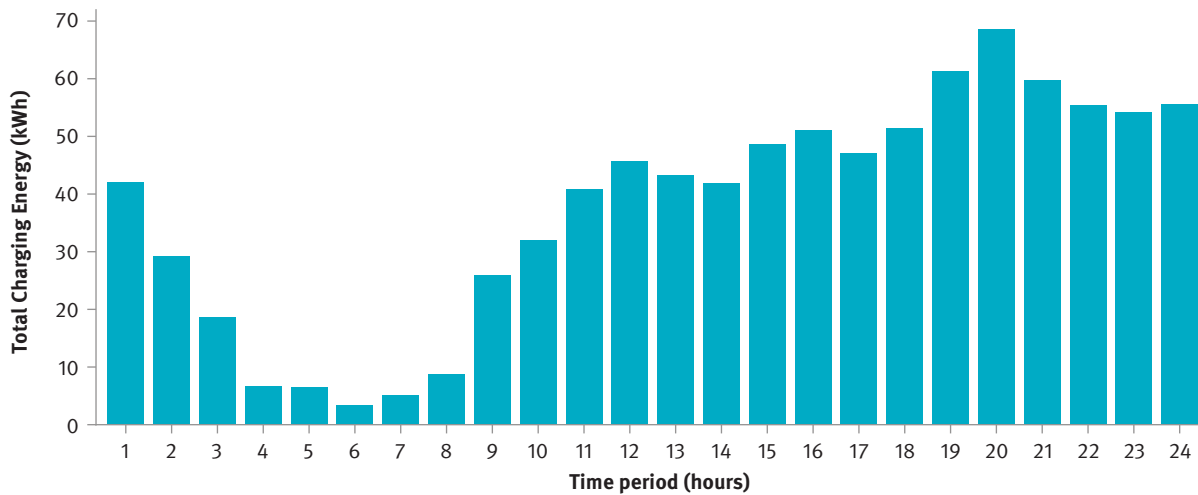


Figure 9: Total aggregated charging energy for all charging events for each hour in the day

After merging the BMS and GPS datasets, the locations of the charging events were categorised as either happening at a battery swap station (BSS) or away from a BSS. The resulting charging energy for each hour in the day, split by charging location, is shown in Figure 10.

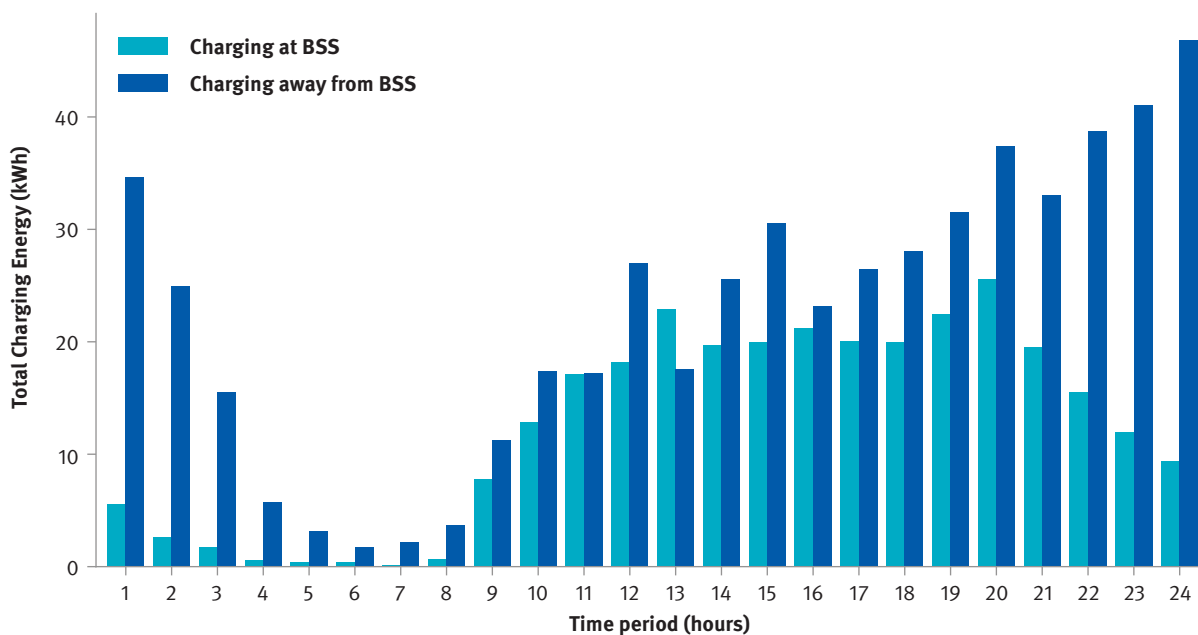


Figure 10: Total aggregated charging energy for each hour in the day split by charging location

As shown in Figure 10, the charging energy at BSSs has a similar distribution to the swapping probabilities shown in Figure 7, since the swapped batteries begin to charge as soon as they are placed in the BSS, until they reach 100% SOC. The distribution of charging energy for charging away from the BSS (i.e., at home or other locations where riders may use personal chargers) shows a relatively similar distribution to the BSS charging during the day, but continues to increase in the evening hours, reaching a peak at midnight, before gradually decreasing to a minimum at around 6:00. This shows that riders with personal chargers make use of overnight charging for their batteries, which results in a different energy profile to that of BSSs.

Co-ordinated charging scenario for BSSs

A hypothetical co-ordinated charging scenario where charging of batteries at BSSs was shifted to off-peak times away from the evening peak demand period was created, as shown in Figure 11.

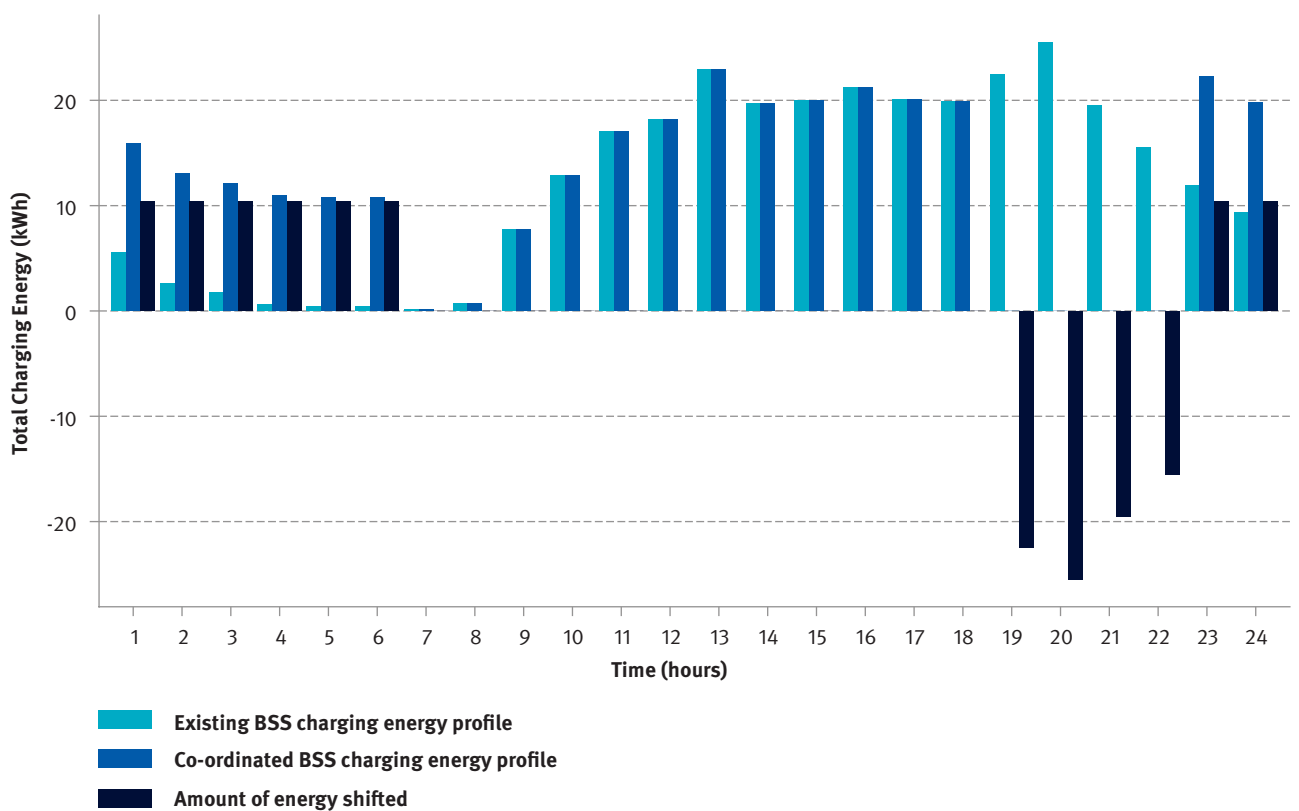


Figure 11: Co-ordinated charging scenario energy profile

For this scenario, all charging at the BSS that would have occurred between 18:00 and 22:00 was shifted (the shifted energy is shown in navy) and distributed evenly between the remaining off-peak hours between 22:00 and 6:00 the following morning. The resulting co-ordinated charging energy profile is shown in blue, compared to the original profile in teal. Note that this BSS charging scenario may not be feasible in practice, and further work would be required to determine how much of the charging at a BSS can feasibly be shifted to off-peak hours, without having an impact on the riders that may need to swap out batteries during this time. Therefore, this scenario illustrates the maximum amount of energy that could be shifted from the evening peak to the off-peak periods.

Swap battery charging emissions analysis

The estimated charging emissions for all charging and for BSS specific charging, aggregated for each half-hour in the day, can be seen in Figure 12 and Figure 13, respectively.

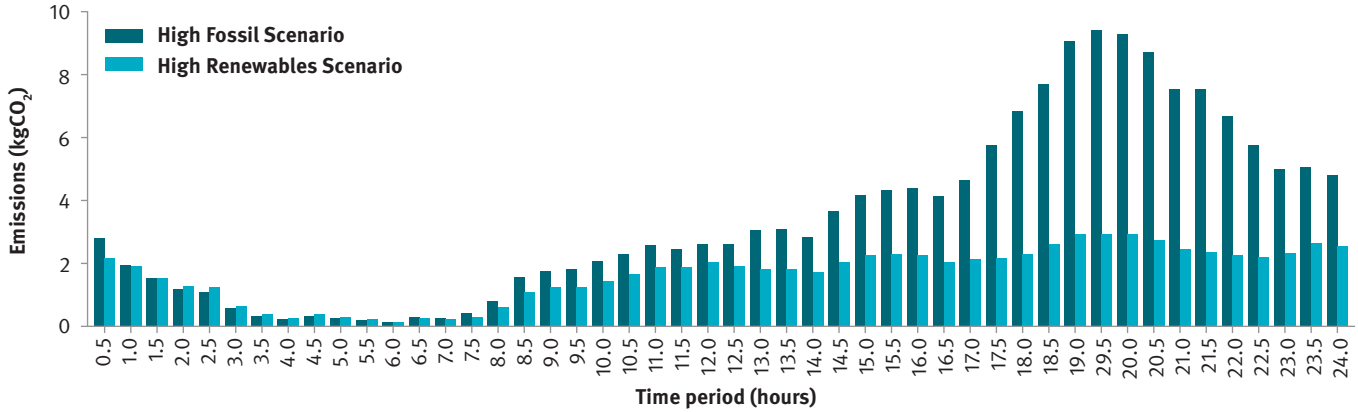


Figure 12: Charging emissions for all charging events aggregated for each half-hour in the day

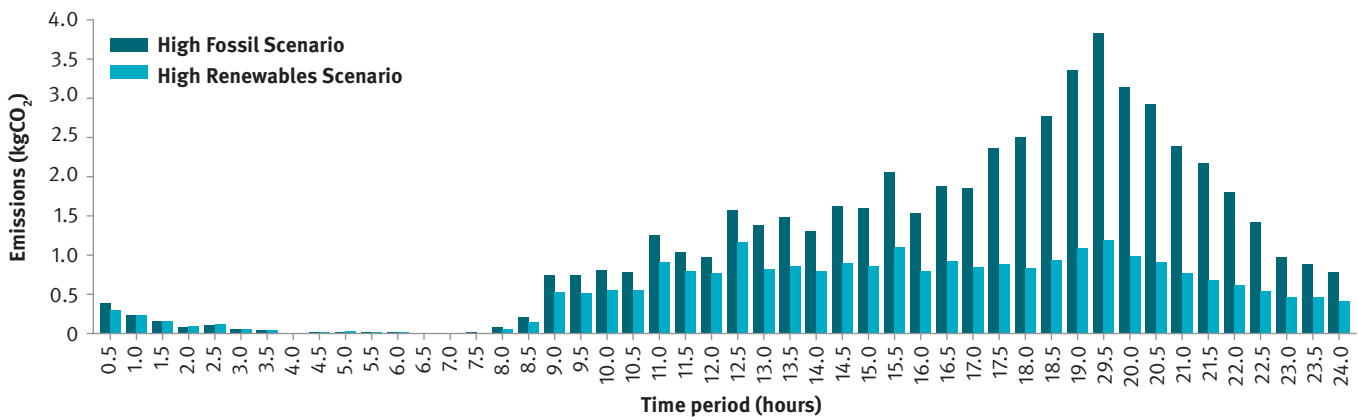


Figure 13: BSS specific charging emissions aggregated for each half-hour in the day

As seen in both figures, the High Fossil Scenario results in higher emissions than the High Renewables Scenario, especially in the evening when emissions rise to a peak between 19:00–19:30. This is due to the higher average emissions factors of the High Fossil Scenario during those hours, as seen earlier in Figure 3, where the mix of fossil-fuelled power plants increases to meet the peak evening power demand.

Next, the estimated emissions for the co-ordinated charging scenario are shown in Figure 14 and Figure 15.

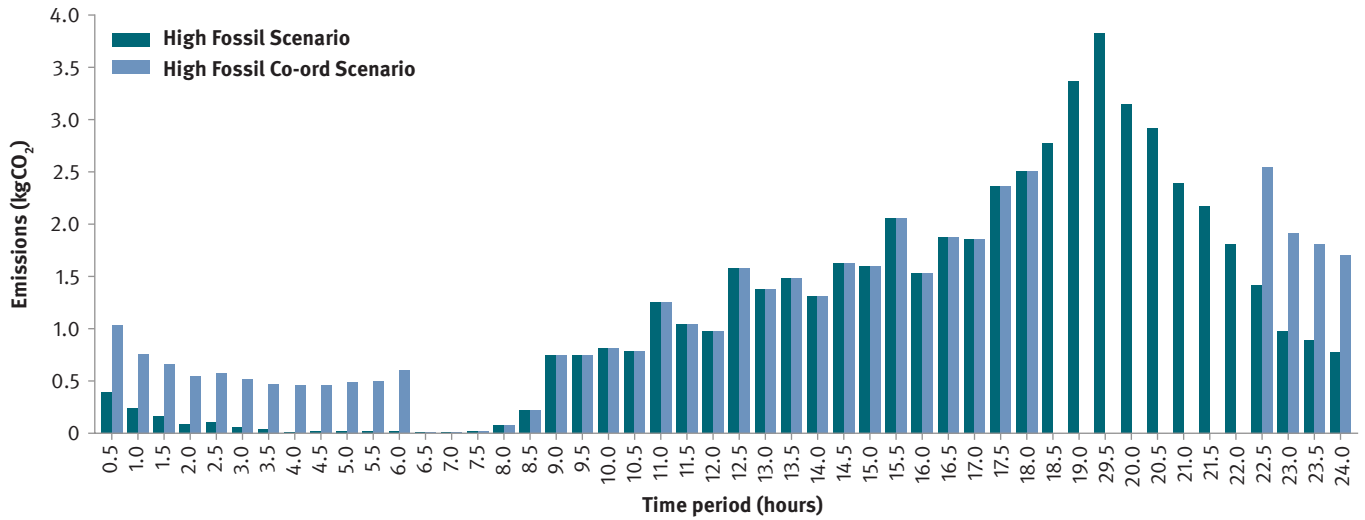


Figure 14: BSS specific High Fossil Scenario charging emissions with and without co-ordinated charging

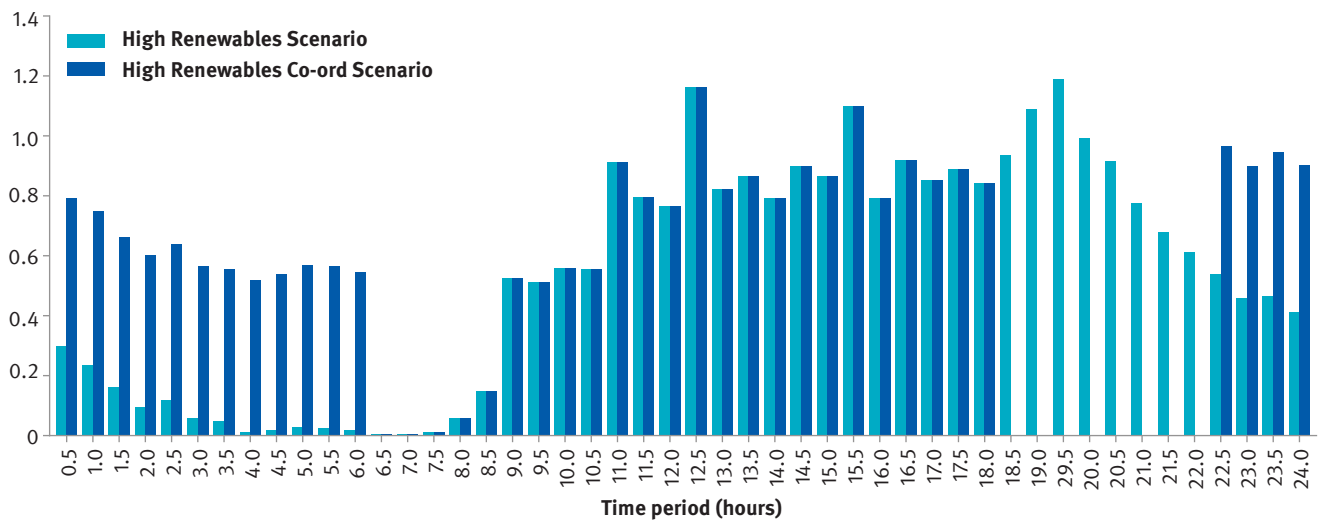


Figure 15: BSS specific High Renewables Scenario charging emissions with and without co-ordinated charging

As shown in the figures, all emissions during the evening peak hours (18:00–22:00) for the charging co-ordinated scenarios are reduced to zero, and the emissions during the off-peak hours that follow are increased compared to the scenarios without charging co-ordination. The total amount of emissions for each scenario can be seen in Figure 16.

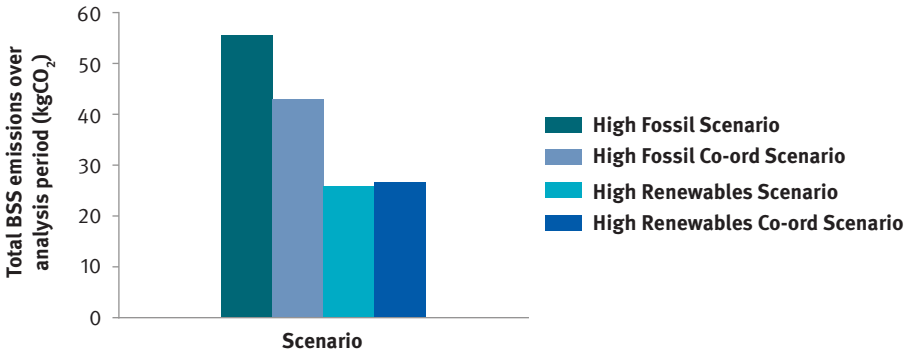


Figure 16: Total estimated emissions over analysis period for all scenarios

The resulting emissions factors for e-motorcycles (gCO₂/km) based on BSS charging emissions and estimated distances driven are detailed in Table 2 and shown in Figure 17.

Table 2: Comparison of emissions factors for ICE and e-motorcycles based on BSS charging for all scenarios

Scenario	EF (gCO ₂ /km)	EF compared to ICE2W baseline	EF compared to un-coordinated scenario
ICE2W Baseline [11]	69.1	-	-
E2W High Fossil	8.44	- 87.8 %	-
E2W High Fossil with co-ord. charging	6.52	- 90.6 %	- 22.7 %
E2W High RE	3.93	- 94.3 %	-
E2W High RE with co-ord. charging	4.06	- 94.1 %	+ 3.3 %

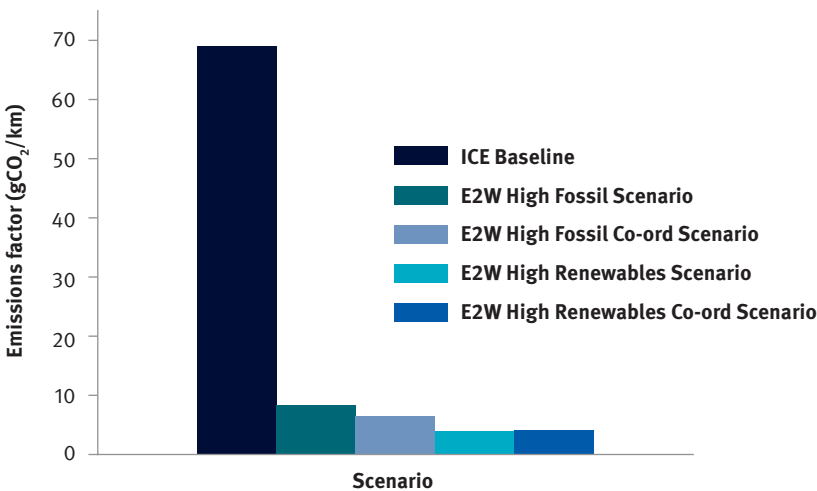


Figure 17: Comparison of emissions factors for ICE and e-motorcycles based on BSS charging for all scenarios

Compared to Internal Combustion Engine (ICE) motorcycles, the e-motorcycles' emissions factors (EF) for all scenarios are substantially lower, with decreases in the range of -87.8 % (E2W High Fossil Scenario) to -94.3 % (E2W High Renewables Scenario). For the High Fossil Scenario, the emissions factor was decreased by 22.7 % by implementing charging co-ordination, which shows the benefit that charging co-ordination could have on days with higher fossil energy in the mix. For the High Renewables Scenario, the emissions factor increased very slightly by 3.3 %, since the AEF is slightly higher in the early hours of the morning, as seen in Figure 3.

Swap battery charging electricity tariff costs

Similar to the calculation of emissions, the electricity costs were determined for each hour in the day based on the tariff scenarios, and the additional co-ordinated charging scenario. The estimated electricity costs from charging for each hour in the day at a BSS are shown in Figure 18.

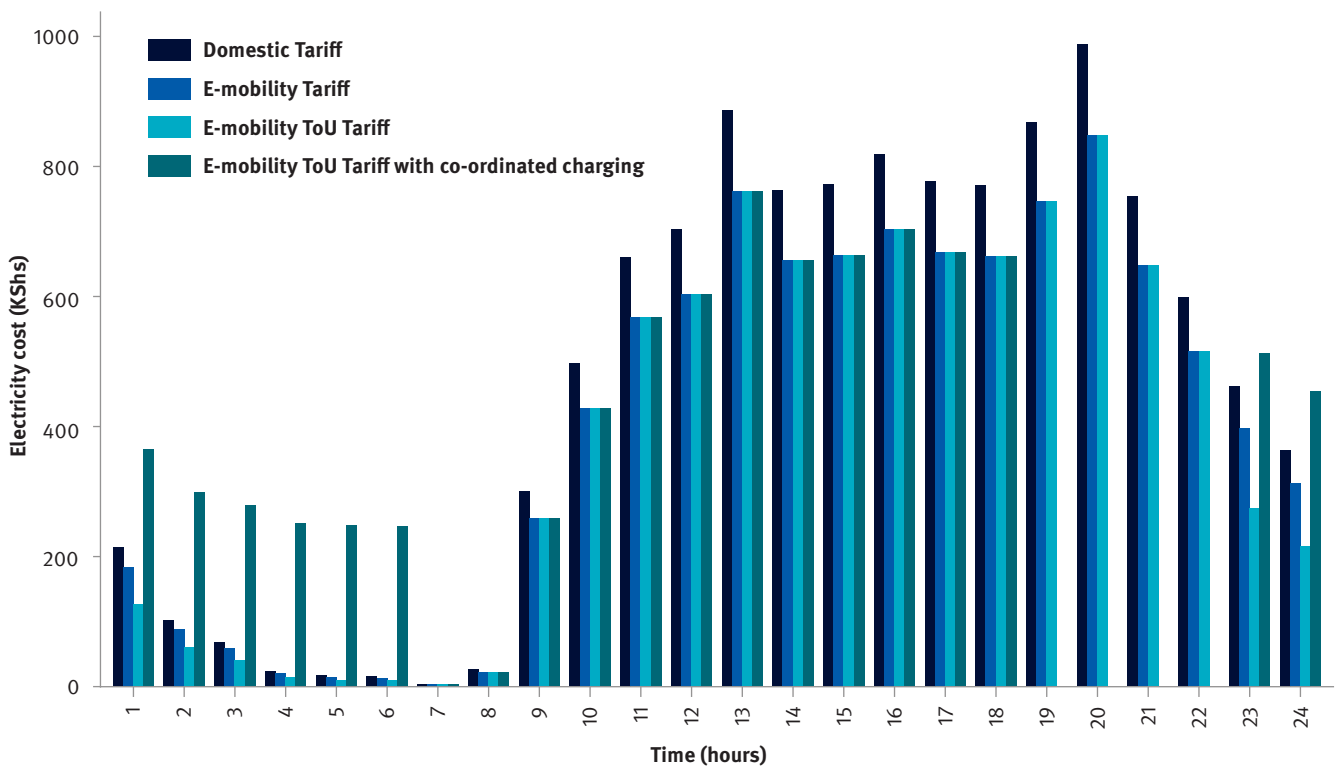


Figure 18: Estimated electricity costs from charging for each hour in the day at a BSS for all scenarios

The figure shows the costs of electricity in the peak period of the co-ordinated charging scenario are reduced to zero, and shifted to the off-peak hours where the electricity is cheaper due to the E-mobility TOU Tariff. To compare these different tariff scenarios, the resulting average electricity costs for BSS charging are detailed in Table 3 and shown in Figure 19 for all scenarios.

Table 3: Comparison of average electricity costs at BSS for all scenarios

Scenario	Average Elec Cost (KShs/kWh)	Cost compared to domestic tariff	Cost compared to un-coordinated scenario
Domestic Tariff	38.69	-	-
E-mobility Tariff	33.25	-16.4 %	-
E-mobility TOU Tariff	32.11	-20.5 %	-
E-mobility TOU Tariff with co-ordinated charging	29.23	-32.4 %	- 9.0 %

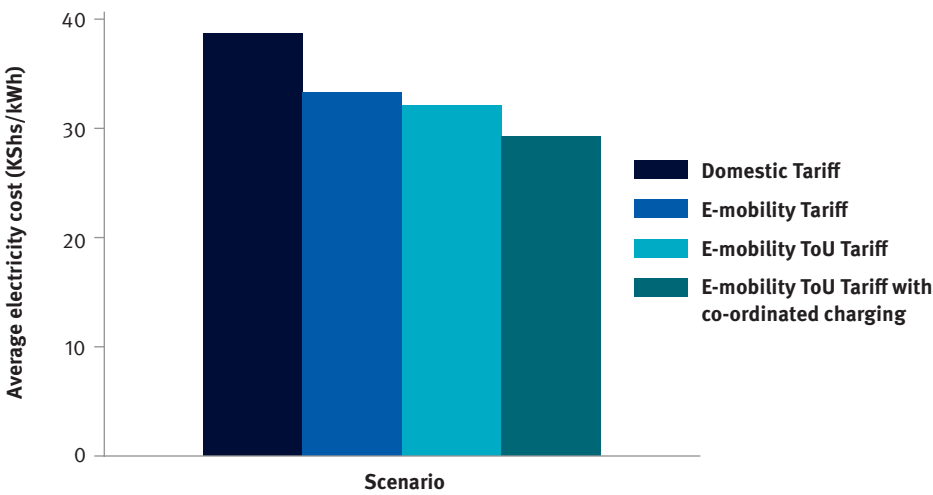


Figure 19: Comparison of average electricity costs at BSS for all scenarios

The results show that the E-mobility Tariff Scenario provides savings of 16.4 % compared to the Domestic Tariff Scenario. If an E-mobility TOU Tariff was implemented, and the BSSs were able to co-ordinate their charging, this would lead to almost double the savings at 32.4 % compared to the domestic tariff. If an E-mobility TOU Tariff was introduced, the difference between average electricity costs between un-coordinated and co-ordinated charging to make use of the off-peak tariff is 9.0%. The TOU tariff would act as an incentive to shift load away from the peak if BSSs are able to practically implement the amount of charging co-ordination required.

Optimal number of swap stations and batteries

The battery swapping system simulation [6], [7] was run with the inputs shown in Table 4, below.

Table 4: Input values for battery swapping simulation

Input	Value
N_{E2W}	200
$N_{batt/BSS}$	11
P_{charge} (kW)	0.73
C_{batt} (kWh)	2.1
$N_{swaps/user/day}$	1.56
N_{BSS}	6 to 16 (step of 2)

The reliability results from the battery swapping simulation for the different numbers of battery swap stations and their corresponding battery ratios are showing in Figure 20 and Figure 21 below.

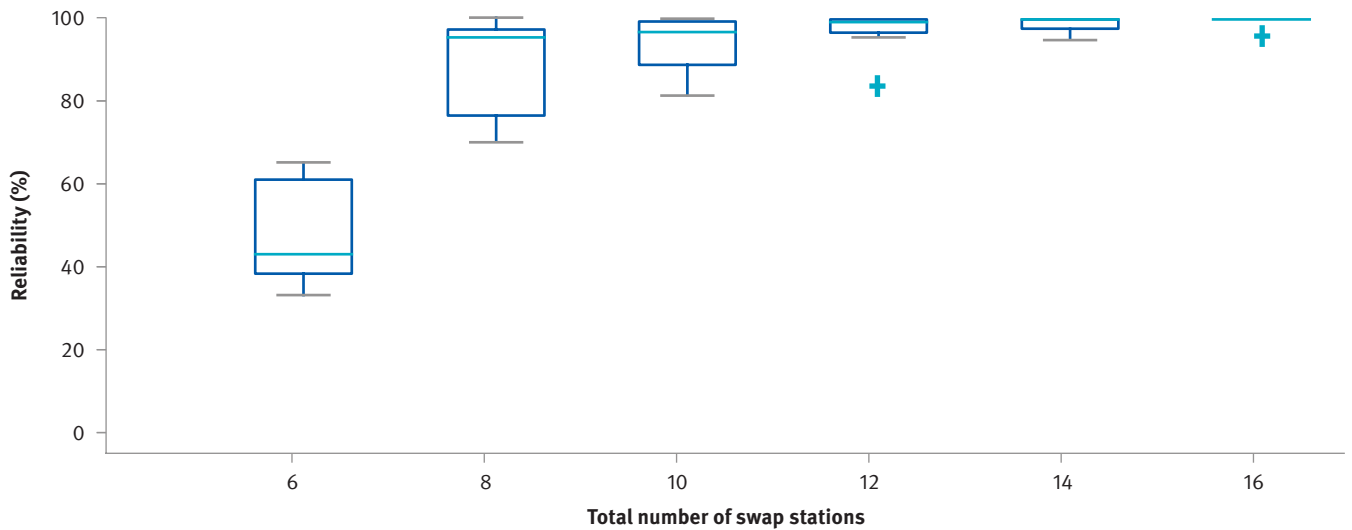


Figure 20: Boxplots of reliability vs total number of swap stations for 200 simulated E2Ws

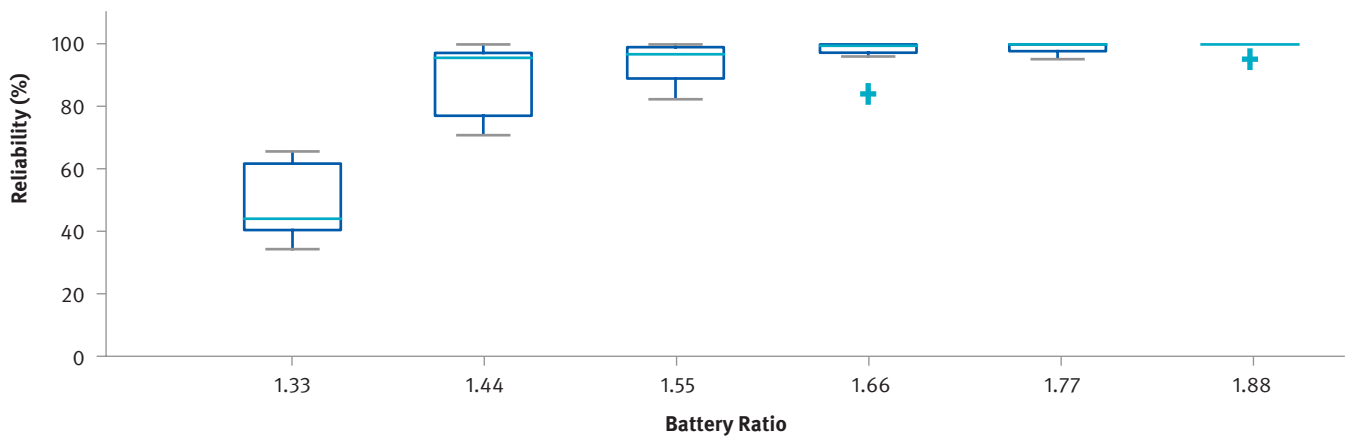


Figure 21: Boxplots of reliability vs battery ratio for 200 simulated E2Ws

As shown in these boxplots, the range of reliabilities for the swap stations in each simulated scenario increases as the number of stations/battery ratio increase. After 12 swap stations, or a battery ratio of 1.66 in this scenario, the increase in reliability for each successive increase in swap stations is almost negligible. Therefore, for swap cabinets with the specifications as set out in Table 4, an optimal battery ratio would be approximately 1.66. Based on a battery ratio of 1.66, the number of BSSs required for various number of E2Ws were determined as shown in Table 5.

Table 5: Estimated number of BSS required for various numbers of E2Ws

No. of E2Ws	Estimated no. of BSSs required
100	6
200	12
500	30
1 000	60
2 000	120
5 000	300
10 000	600
20 000	1200
50 000	3000

As noted above, varying any of the simulation inputs, such as power rating, number of batteries, battery capacity, or number of swaps per user per day, would lead to different reliability results for different battery ratios. This makes it difficult to generalise any results for optimal battery ratios in different swap station systems. For the system simulated here, an optimal battery ratio of 1.66 results in 6 BSSs required for every 100 e-motorcycles.

Optimal locations of swap stations based on vehicle trip data

The analysis area (Nairobi + buffer) was partitioned into 8 718 hexagonal bins using an H3 [14] resolution of 9, as shown in Figure 22. For H3 resolution 9, each hexagon measures 302 m across flats (AF) and has an average area of 0.116 km² [14]. Lower H3 resolutions can also be used to increase the size of the hexagons used to partition the area. Note that the region of Nairobi National Park was removed from the analysis area to reduce the total number of hexagons to solve for in the optimisation, with the assumption that no BSSs would be placed there.

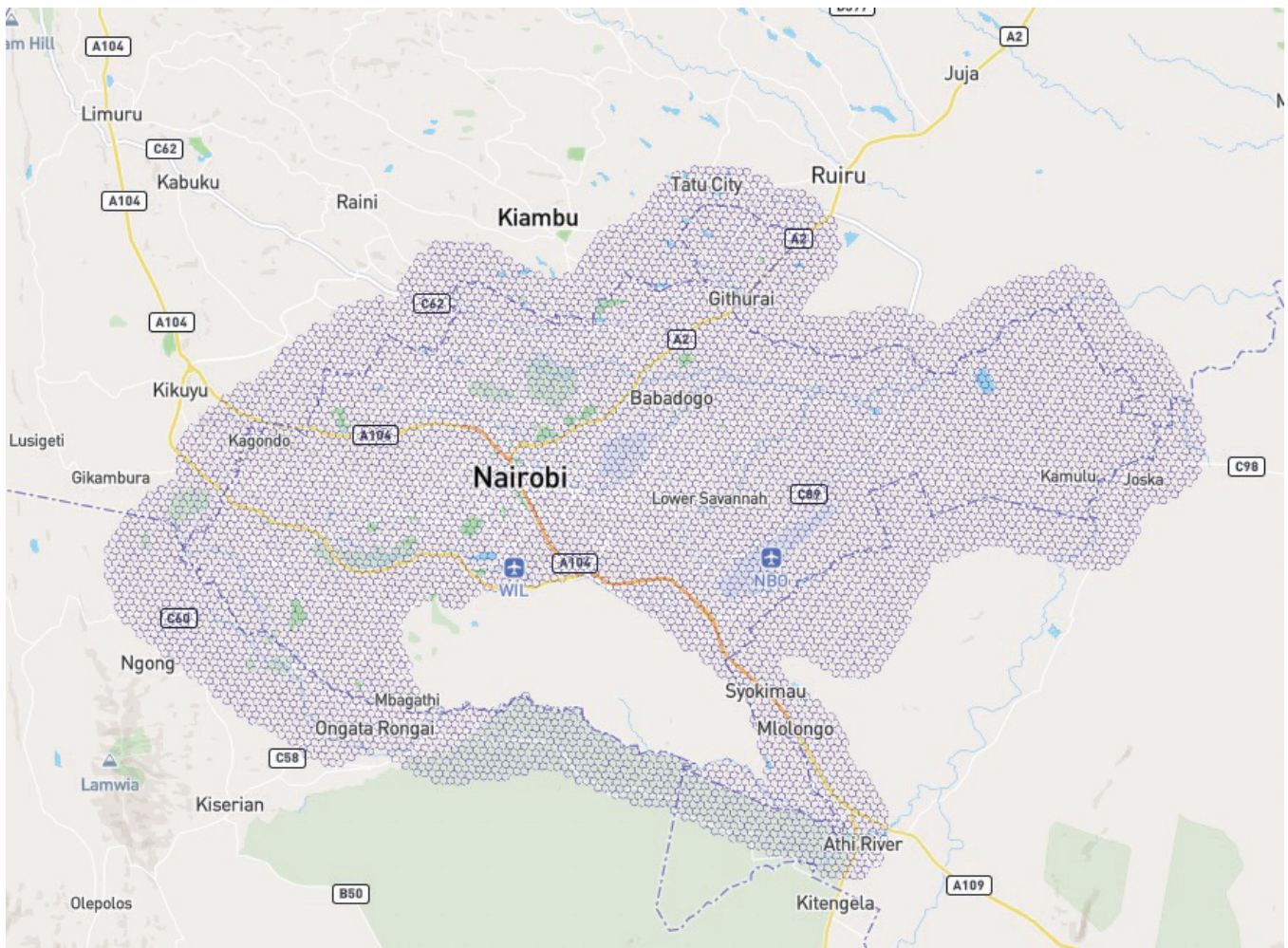


Figure 22: Analysis area converted to hexagonal bins. Map created using Kepler.gl [15], Mapbox [16] and OpenStreetMap [17].

The trip counts were then aggregated into the hexagonal bins to determine regions more likely to have higher battery swapping demand, as shown in the heat map in Figure 23. Note that the heatmap colours are based on quantile ranges. Trip counts less than 10 were not included so that regions with a small number of trips would not be shown.

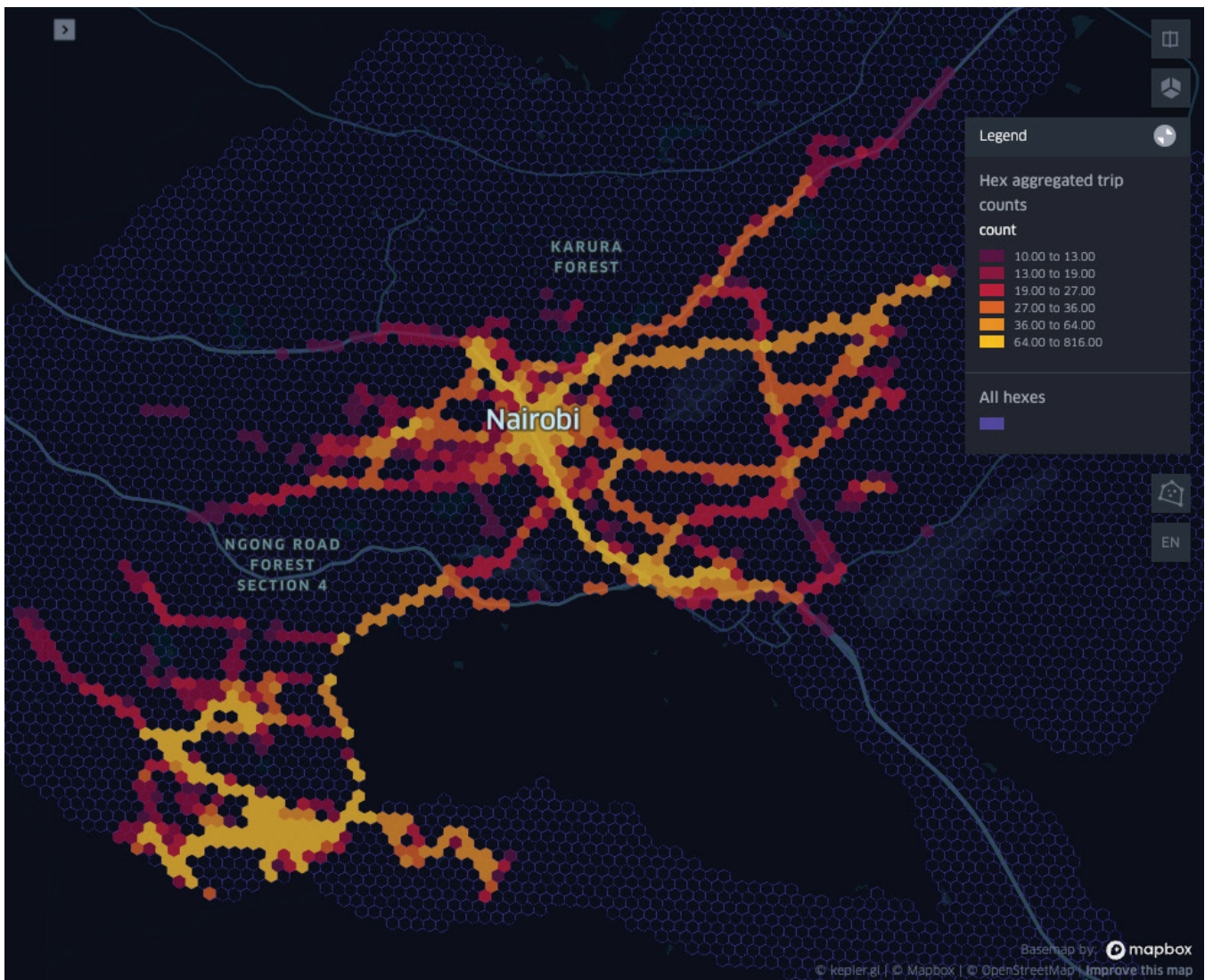


Figure 23: Heat map of aggregated trip counts. Map created using Kepler.gl [15], Mapbox [16] and OpenStreetMap [17].

As shown in Figure 22, the areas with highest trip counts for this dataset are around Nairobi CBD and the Ongata Rongai region in the Southwest. Higher trip counts also appear along major roads around these regions.

The BSS region optimisation was then run for three hypothetical BSS deployment stages, using the inputs shown in Table 6 for each stage.

Table 6: Input parameters for 3 stage BSS location optimisation

Input	Stage 1	Stage 2	Stage 3
R	10	10	10
M	1.0	1.0	1.0
w_0	1.0	1.0	1.0
w_1	0.5	0.5	0.5
w_2	0.3	0.3	0
w_3	0.2	0.2	0
w_4	0.1	0	0
w_5	0.05	0	0

The coverage weights ($w_0 - w_5$) are used in the optimisation to set coverage and spacing constraints related to neighbouring hexagon regions (see Appendix A for more details). The values were changed for each stage of the optimisation to gradually allow the successive BSS locations to be closer to each other by setting the outer ring weights to zero, starting with a minimum distance of 5 hexagonal bins (~1.5 km AF) between them, and then going down to a minimum of 3 (~0.9 km AF) and then 1 (~0.3 km AF) between them for the third stage. Note that the coverage weights w_1 to w_5 are successively reduced to reduce the weighting of neighbouring hexagons that are further away, as the BSS is assumed to meet the demand of the region its placed in, while meeting only a set portion of the demand in each neighbouring region. Figure 24 shows how the coverage weights are distributed around a selected hexagon for BSS placement with five neighbouring hexagon rings.

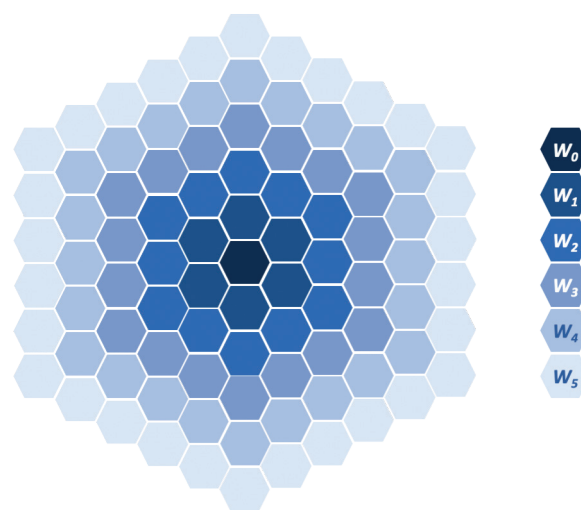


Figure 24: Coverage weight distribution for a hexagon with 5 neighbouring hexagon rings

The three-stage scenario described here is for illustrative purposes, as the optimisation parameters can be set according to the requirements of the BSS planner, including their assumptions for the level of demand that the BSSs will cover. The results showing the optimal regions selected for new BSSs for each stage are shown in Figure 25, with a close-up of the results for central Nairobi shown in Figure 26.



Figure 25: Three-stage BSS location optimisation results for Nairobi. Map created using Kepler.gl [15], Mapbox [16] and OpenStreetMap [17].

As shown in Figure 24 and Figure 25, the existing BSS locations are also considered in the analysis and their locations are shown as regions with white borders. The optimisation has located 10 new BSSs in each stage, according to the constraints set, in areas with higher combined scores. As shown, the minimum distance (number of hexagons) between BSS regions in each successive stage is reduced as per the input parameters. As these results are based on a relatively small dataset, the results are expected to differ when larger, more representative, datasets are available for analysis. However, these results illustrate the process of using the optimisation model for determining optimal regions for new BSS locations in Nairobi.

As described in the Methodology section, after using the optimisation to determine optimal regions for the deployment of BSSs, the BSS planner would then need to perform a detailed site selection process within each region. If any regions are found to be infeasible for siting a BSS, the optimisation process could potentially be rerun with those regions excluded.

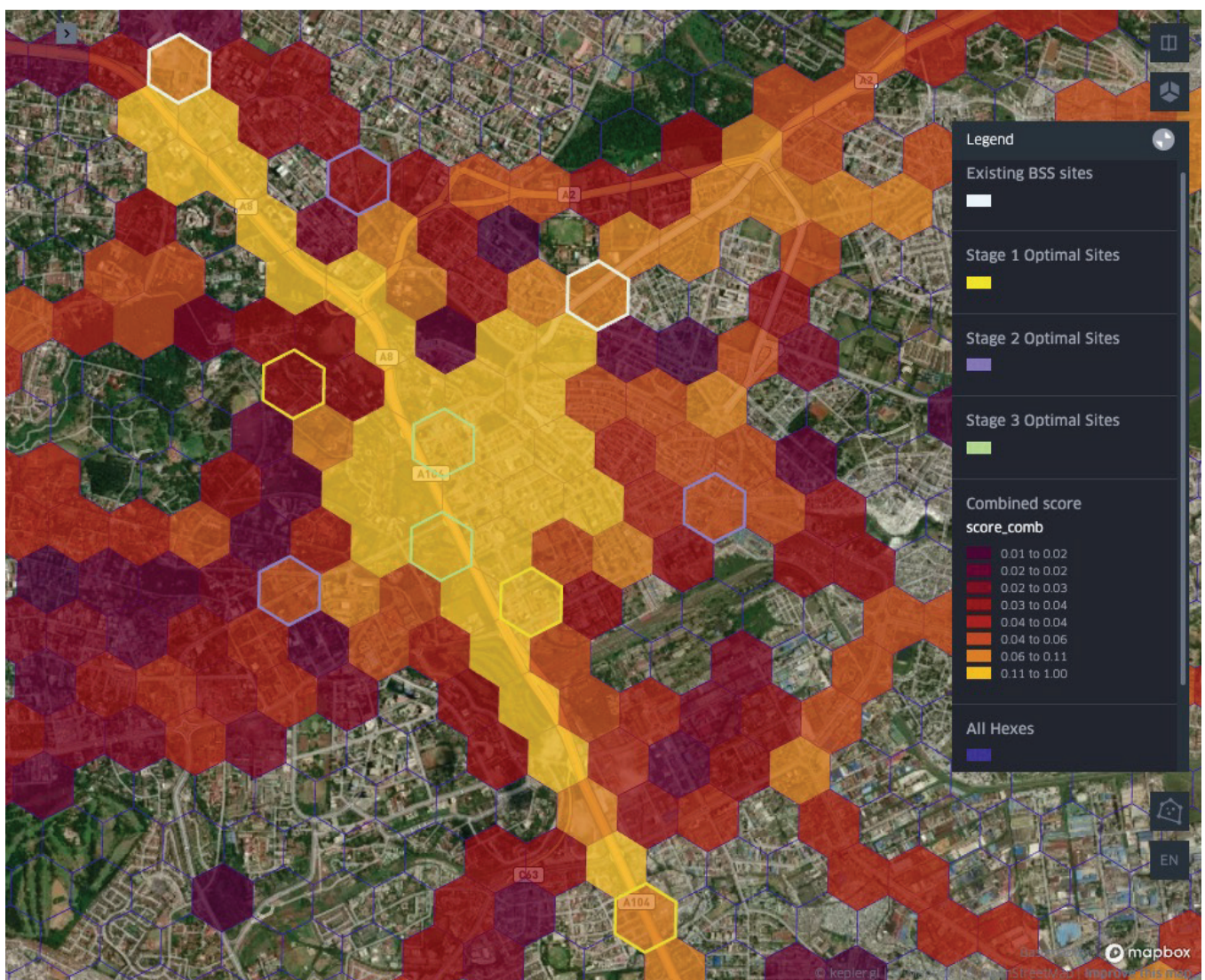


Figure 26: Three-stage BSS location optimisation results – close-up of Nairobi central. Map created using Kepler.gl [15], Mapbox [16] and OpenStreetMap [17].

Conclusions

This report detailed various analyses that were performed using real data from e-motorcycle swap batteries in the city of Nairobi, Kenya. These included the analysis of: e-motorcycles trips; battery swapping demand; battery charging energy consumption; a co-ordinated charging scenario; swap battery charging related emissions for a high renewables and high fossil-based energy mix scenario; charging related electricity costs for different tariff scenarios; optimal battery ratios and numbers of swap stations; and optimal regions for new battery swap stations based on trip data.

Key findings

Some key findings from the study are listed below:

- Most trips by e-motorcycles are relatively short and slow, with an average trip length of 4.5 km, and an average speed of 20.1 km/h. The peak time for trips is the period 17:00–18:00, possibly coinciding with the evening commute.
- The riders seem less likely to swap out their batteries during the busiest trip periods (17:00–18:00). When riders do swap out during the peak period, they appear to do so only when the battery state of charge (SOC) is close to reaching zero (normally around 5 % SOC). This is in contrast to swapping behaviour in the mornings, where riders appear to swap out their battery before their shift begins regardless of the battery state of charge, probably so that they can start their day with a fully charged battery.
- Batteries in the dataset were found to be charged at either battery swapping stations (BSSs) or away from BSSs (possibly at home or other locations using a private charger). The charging profiles for these two destination types were found to be different. This is especially apparent in the evenings, where charging events away from BSSs appeared to make use of overnight charging, with a peak in charging energy consumption around midnight.
- Compared to Internal Combustion Engine (ICE) motorcycles, the e-motorcycles' emissions factors (EF) for all scenarios were estimated to be substantially lower, with decreases in the range of -87.8% (E2W High Fossil Scenario) to -94.3% (E2W High Renewables Scenario). For the High Fossil Scenario, the emissions factor was decreased by 22.7% by implementing charging co-ordination, which shows the benefit that charging co-ordination could have on days with higher fossil energy in the mix.
- The proposed E-mobility Tariff Scenario (non-TOU) provides savings of 16.4% compared to the Domestic Tariff Scenario. If an E-mobility TOU Tariff was implemented, and the BSSs were able to co-ordinate their charging, this would lead to almost double the savings at 32.4% when compared to the domestic tariff. This increased reduction in total electricity costs could act as an incentive for BSS operators to attempt to co-ordinate their charging if the TOU tariff was in place.
- For swap cabinets with the chosen specifications for this study, an optimal battery ratio would be approximately 1.66 batteries (total system) for every e-motorcycle. This would mean approximately 6 BSSs for every 100 e-motorcycles if every BSS contained 11 batteries in storage.
- The BSS location optimisation model can be used to determine optimal regions for BSS sites in a multi-stage deployment strategy based on trip location data. Optimisation parameters can be adjusted for each deployment stage, to allow different spacing and coverage constraints for each solution.

Further work

There are several areas that have been identified where further work could be done to build upon the analysis methodology and models developed during this study, as detailed below:

- The analysis provided in this report is based on a relatively small dataset (small number of devices and 3-month data collection period), however, it is hoped that the analysis methodology developed here can be applied to larger datasets in future as they become available.
- Interviews or surveys of e-motorcycles riders about their choices related to battery swapping could provide insight into the swap and SOC distributions for different times in the day.
- The half-hourly average emissions factor estimation for Kenya's grid could be improved if more data were to be made available from Kenya's electricity companies, such as KenGen and KPLC. Marginal emissions factors at different time periods could also be determined if access to more detailed electricity demand data were to be provided.
- The methodology is adaptable to different regions, so analyses can also be done in other cities that use e-motorcycles and battery swapping systems.
- The methodology allows areas to be excluded from the analysis, as was done for the Nairobi National Park. Future work could look at excluding additional areas within the analysis region that are not appropriate for BSSs, such as regions where motorcycles are banned or where local planning prevents the installation of this type of infrastructure.
- Certain aspects of the analysis could be adapted to other types of electric vehicles, such as electric 4-wheelers or buses, if they are able to produce similar location and battery analytics data.
- The current methodology can determine stopping locations of vehicles, which could potentially be used to optimise regular charging station regions using the optimisation model. However, the analysis currently has no way of differentiating whether stops are happening at locations that might reveal sensitive information (such as home locations of riders) or at public locations that could be used as potential charge sites. Therefore, these stopping locations were not used as part of the analysis. Further work could be done to remove sensitive stop locations from the dataset, so that the data could be used for charging station region optimisation.
- Grid infrastructure data could be included in the analysis if detailed data becomes available, such as available capacity or constraints at substations, transformers, distribution networks and transmissions lines in the region. This data could be used to optimise the locations to make use of available capacity and avoid areas that are experiencing constraints.
- Projections of EVs in the regions could be used to analyse various future scenarios.

To maximise the potential future utility of the analysis framework developed in this study, the models have been made openly available for e-mobility stakeholders to use and adapt the methodology [18]. Please cite this report and the appropriate release version of the analysis model when using the analysis framework in other research or work.

Suggested citation: Sheehan, C. and Green, T.C. (2023) *ChargeUp! Data Swap! Using data from battery swapping e-motorcycles in Nairobi to assess impacts and plan infrastructure*. Imperial College London.

References

- [1] AEMDA, “E-mobility Country Profile 2022: Kenya,” 2022. [Online]. Available: www.aemda.org
- [2] Shell Foundation, “Financing the transition to electric vehicles in sub-Saharan Africa,” 2022.
- [3] C. Chen and G. Hua, “A New Model for Optimal Deployment of Electric Vehicle Charging and Battery Swapping Stations,” *International Journal of Control and Automation*, vol. 7, no. 5, pp. 247–258, 2014, doi: [10.14257/ijca.2014.7.5.27](https://doi.org/10.14257/ijca.2014.7.5.27).
- [4] K. A. Collett, M. Byamukama, C. Crozier, and M. Mcculloch, “Energy and Transport in Africa and South Asia: State of knowledge paper,” 2020.
- [5] R. Pagany, L. Ramirez Camargo, and W. Dorner, “A review of spatial localization methodologies for the electric vehicle charging infrastructure,” *International Journal of Sustainable Transportation*, vol. 13, no. 6. Taylor and Francis Ltd., pp. 433–449, Jul. 03, 2019. doi: [10.1080/15568318.2018.1481243](https://doi.org/10.1080/15568318.2018.1481243).
- [6] C. S. Sheehan, T. C. Green, and N. Daina, “Enabling e-Mobility in Africa: A Techno-Economic Study of Battery Swap Options for e-Motorcycle Taxis,” M.Sc. thesis, Imperial College London, 2020.
- [7] C. S. Sheehan, T. C. Green, and N. Daina, “A Simulation Approach to Analyse the Impacts of Battery Swap Stations for e-Motorcycles in Africa,” in *IEEE AFRICON Conference*, Institute of Electrical and Electronics Engineers Inc., Sep. 2021. doi: [10.1109/AFRICON51333.2021.9570895](https://doi.org/10.1109/AFRICON51333.2021.9570895).
- [8] ARC Ride, “ARC Ride: Energising a transport revolution,” 2021. <https://www.arcrideglobal.com/#/home> (accessed Aug. 06, 2021).
- [9] A. Graser, “MovingPandas: Efficient structures for movement data in Python,” *GI_Forum*, vol. 7, no. 1, pp. 54–68, 2019, doi: [10.1553/GISCIENCE2019_01_S54](https://doi.org/10.1553/GISCIENCE2019_01_S54).
- [10] J. Ngumi *et al.*, “Report of the Presidential Taskforce on the Review of Power Purchase Agreements (PPAS),” 2021.
- [11] B. Notter, F. Weber, J. Füssler, and U. Eichhorst, “Updated Transport Data in Kenya 2018,” 2019. Accessed: Apr. 01, 2020. [Online]. Available: www.changing-transport.org/country/kenya/
- [12] KPLC, “Abridged version of the retail tariff application to the Energy and Petroleum Regulatory Authority,” 2023.
- [13] J. Asamer, M. Reinthaler, M. Ruthmair, M. Straub, and J. Puchinger, “Optimizing charging station locations for urban taxi providers,” *Transp Res Part A Policy Pract*, vol. 85, pp. 233–246, Mar. 2016, doi: [10.1016/j.tra.2016.01.014](https://doi.org/10.1016/j.tra.2016.01.014).
- [14] Uber Technologies, “H3 Hexagonal hierarchical geospatial indexing system,” 2023. <https://h3geo.org/> (accessed Mar. 27, 2023).
- [15] Uber Technologies, “Kepler.gl,” 2018. <https://kepler.gl/> (accessed Mar. 28, 2023).
- [16] MapBox, “Build Dynamic Maps with Mapbox,” 2023. <https://www.mapbox.com/about/maps/> (accessed Mar. 28, 2023).
- [17] OpenStreetMap Foundation, “OpenStreetMap,” 2023. <https://www.openstreetmap.org/copyright> (accessed Mar. 28, 2023).
- [18] C. Sheehan, “Cameron-Sheehan/ChargeUp-Data-Analysis: Initial release,” Apr. 2023, doi: [10.5281/ZENODO.7869160](https://doi.org/10.5281/ZENODO.7869160).

- [19] A. Rohatgi, “WebPlotDigitizer: Version 4.6,” 2022. <https://automeris.io/WebPlotDigitizer/index.html> (accessed Mar. 30, 2023).
- [20] I. Thain and R. Bertani, “Geothermal power generating plant CO₂ emission survey,” *IGA news*, vol. 49, pp. 1–3, 2002.
- [21] CDM, “PSB0055: Grid Emission Factor for the Republic of Kenya - Third Submission,” 2020. https://cdm.unfccc.int/methodologies/standard_base/2015/sb145.html (accessed Mar. 20, 2023).
- [22] S. Shah, “Historic electricity cost data for Kenya,” 2023. <https://www.stimatracker.com/historic#tariffs> (accessed Mar. 16, 2023).
- [23] J. S. Roy and S. A. Mitchel, “PuLP,” 2005. <https://pypi.org/project/PuLP/> (accessed Mar. 27, 2023).
- [24] J. Jasper, “Cutting battery industry’s reliance on cobalt will be an uphill task,” *The Guardian*, 2020. <https://www.theguardian.com/environment/2020/jan/05/cutting-cobalt-challenge-battery-industry-electric-cars-congo> (accessed Feb. 01, 2023).

Appendix A – Additional Methodology Details

Calculation of half-hourly emissions factors for the Kenyan grid

First, representative day energy mix profiles for Kenya were sourced from the 2021 Report of the Presidential Taskforce on the Review of Power Purchase Agreements (PPAS) [10]. Two energy mix profiles were provided in the report, one for a day with high renewables availability, and one with low renewables availability (i.e. high fossil). The report noted that the high fossil scenario occurs on about 5 days annually in Kenya. Data points were extrapolated for every half-hour from the graphs in the report using the WebPlotDigitizer tool [19] for use in this analysis. The resulting demand profiles for each scenario are shown in Figure 27 and Figure 28.

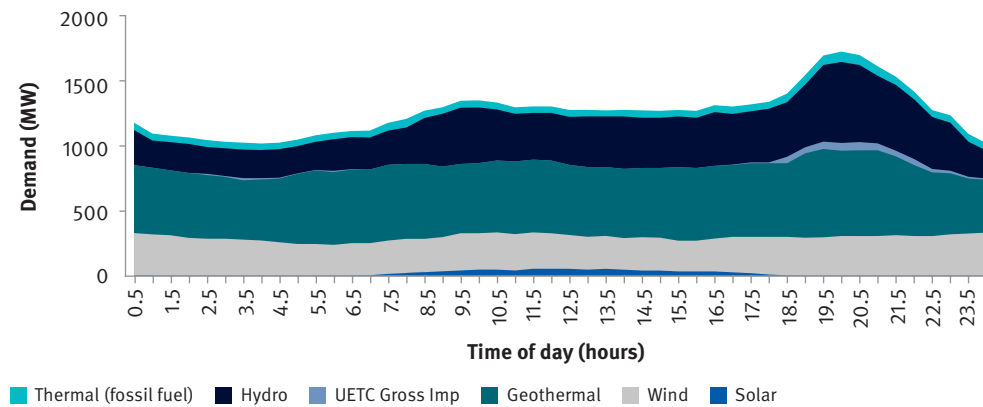


Figure 27: Kenyan day demand profile (high renewables scenario). Adapted from [10]

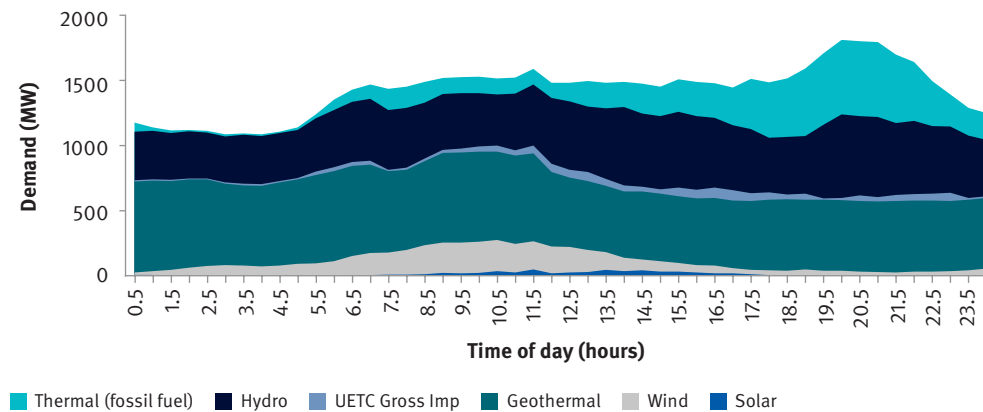


Figure 28: Kenyan day demand profile (high fossil scenario). Adapted from [10]

The energy mix profiles were then used to determine the percentage of each energy source at each half-hourly period in the day. The resulting energy mix in percentage terms are shown in Figure 29 and Figure 30.

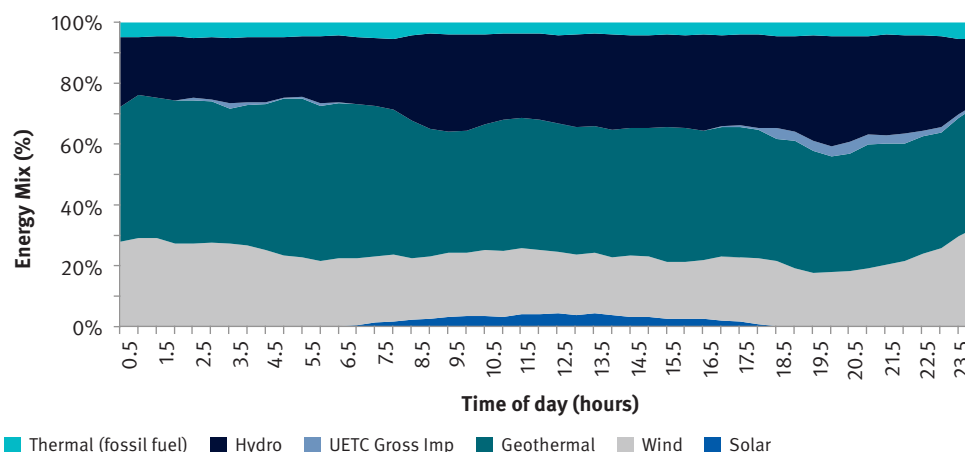


Figure 29: Kenyan day energy mix (high renewables scenario)

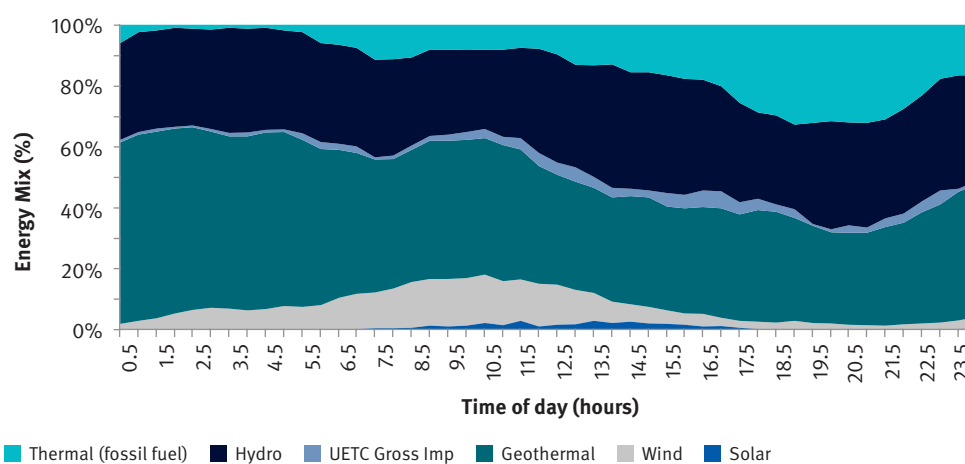


Figure 30: Kenya day energy mix (high fossil scenario)

The emissions factors (EFs) assumed for each energy source are summarised in Table 7.

Table 7: Emissions factors assumed for Kenya's energy mix

Energy source	Emissions factor (tCO ₂ /MWh)
Solar	0
Wind	0
Geothermal	0.122 [20]
UETC Gross Imports	0
Hydro	0
Thermal (fossil fuels)	0.650 tCO ₂ /MWh [21]

The most recent data found to be available for the emissions factors of Kenya's fossil fuelled thermal power plants (heavy fuel oil and Kerosene) was for the year 2019 as part of Kenya's submission to the UNFCCC for a CDM standardised baseline grid emissions factor [21]. The data also contained each of the fossil fuelled thermal power plants' total emissions and net electricity output for 2019. These values were used to determine an average emissions factor of 0.650 tCO₂/MWh for fossil fuelled thermal power plants in Kenya. As seen in Figure 29 and Figure 30, Kenya's

energy mix also contains a large portion of geothermal power. No data was found specific to the emissions factors of Kenya’s geothermal power plants, so the international average of 0.122 tCO₂/MWh was used for calculations [20]. Lastly, operational emissions factors for the renewable energy sources of solar, wind, and hydro power were assumed to be zero. Without details on the emissions factors for imported electricity in Kenya available, and with these imports making up a small percentage of the total energy mix, these emissions were not considered in this analysis. The inclusion of emissions from imported electricity is expected to have a small impact on the total calculated emissions, however, the investigation of this is left for future work.

The final step to determine the half-hourly average emissions factors involved multiplication of the emissions factor for each source by the percentage of its contribution to the energy mix and summing these for each half-hour period. This calculation was done for both scenarios to determine half-hourly average emissions factors (AEFs) for the High Renewables Scenario and a High Fossil Scenario. The resulting AEFs are shown in Figure 31 below.

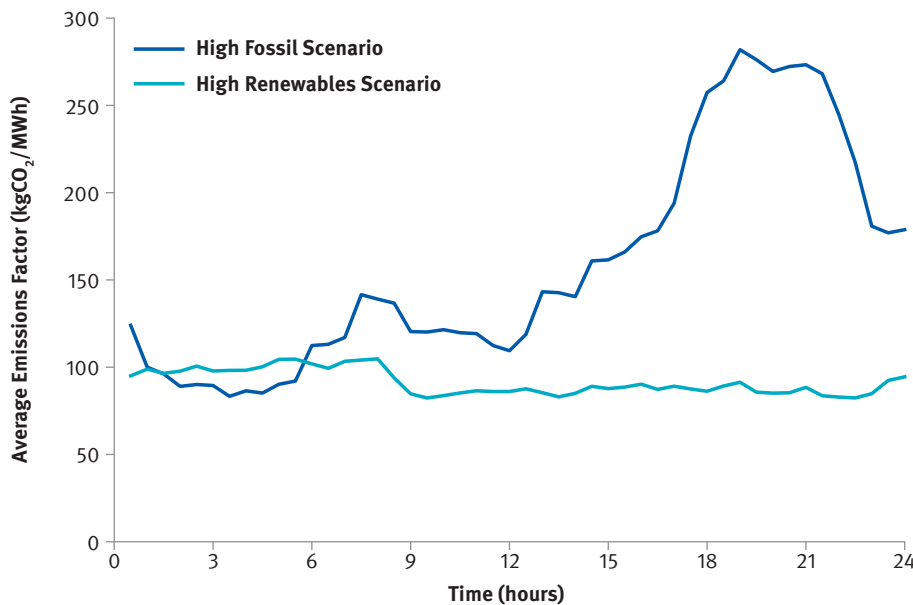


Figure 31: Average emissions factors for the high renewables scenario and high fossil scenario. Source: Author

Swap battery charging electricity tariff scenarios

To investigate different electricity tariffs’ effects on charging costs, different base tariff scenarios were explored, as detailed in Table 8.

Table 8: Base tariffs for each tariff scenario

Tariff scenario	Base tariff during peak hours (KShs/kWh)	Base tariff during off-peak hours (KShs/kWh)
Scenario 1: Domestic [12]	21.50	21.50
Scenario 2: E-mobility [12]	17.00	17.00
Scenario 3: E-mobility TOU*	17.00	8.50

*E-mobility time-of-use tariff scenario developed by authors

The Domestic and E-mobility tariffs are based on the July 2023 tariffs in the Kenya Power and Lighting Company's (KPLC) retail tariff application to the Energy and Petroleum Regulatory Authority (EPRA) [12]. The third scenario was developed by the authors to explore the impact of providing an E-mobility time-of-use (TOU) tariff structure, where the base tariff is discounted at 50% during off-peak hours, as is done with other KPLC TOU tariffs [12].

The following surcharges were also included in the calculation of the electricity costs for charging.

Table 9: Surcharges and taxes for electricity costs

Surcharge type	Surcharge rate [22]	Date of historic variable rate sourced from [22]
Fuel Cost Charge (FCC)	8.3 KShs/kWh (variable)	March 2023
Foreign Exchange Rate Fluctuation Adjustment (FERFA)	2.16 KShs/kWh (variable)	March 2023
Inflation Adjustment (IA)	0.85 KShs/kWh (variable)	March 2023
WARMA Levy	0.01 KShs/kWh (variable)	March 2023
ERC Levy	0.03 KShs/kWh (fixed)	-
REP Levy	5% of base tariff	-
VAT	16% of (base tariff + FCC)	-

With the inclusion of the surcharges the cost of energy for each scenario was determined, as summarised in Table 10.

Table 10: Tariff scenarios summary

Tariff scenario	Hours	Base tariff (KShs/kWh)	Elec cost (KShs/kWh incl. VAT)
Scenario 1: Domestic [12]	Peak	21.50	38.69
	Off-peak	21.50	38.69
Scenario 2: E-mobility [12]	Peak	17.00	33.25
	Off-peak	17.00	33.25
Scenario 3: E-mobility TOU	Peak	17.00	33.25
	Off-peak	8.50	22.96

Optimal regions for swap stations based on vehicle trip data

To determine optimal regions of battery swap stations based on vehicle trip data, a Mixed Integer Linear Programming (MILP) optimisation model was developed and implemented in Python. The methodology was based on the work of [13], where charging station locations were optimised for urban taxi providers, by partitioning the analysis area into a set of hexagons (H). However, for the analysis detailed here, battery swap stations are optimally located instead of charging stations. The method from [13] was adapted as detailed in the methodology below.

Battery swap demand was assumed to correlated with regions that had a higher number of trips that passed through them, since battery swapping could be done within a few minutes on the way to any location. This is different to opportunity charging assumed in study [13], where demand would be located at start/end locations since longer stopping durations would be required to charge. Each hexagon was assigned a transformed value $c_{trips,i} \in [0,1]$, where $i \in H$, based on the number of trips that passed through the hexagons. In addition to the transformed aggregated trip count values, the transformed population density values at each hexagon $c_{pop,i} \in [0,1]$ can also be included in the optimisation using a combined weighted demand score c_i , as shown in Eq. (2) and (3).

$$c_i = W_{trips} c_{trips,i} + W_{pop} c_{pop,i} \quad (2)$$

$$W_{trips} + W_{pop} = 1 \quad (3)$$

The values of the weights ($w_{trips}, w_{pop} \in [0,1]$) can be adjusted to change the level of influence that either of the values has on the choice of optimal sites. Note that for this study, the population weight was set to zero such that aggregated trip counts were the only factor considered to influence demand ($c_i = c_{trips,i}$). Future work might consider what level of population weighting may be appropriate.

The maximum number (n) of neighbouring hexagon rings around each hexagon ($N_{i,k}$), considered when determining demand coverage scores and constraints was increased to five ($n = 5$). This increase allows more options for coverage and spacing constraints when determining optimal BSS site regions. As shown in Figure 23 earlier in the report, a hexagon i is covered with weight $w_o \in [0,1]$ if i itself is selected for placing a BSS, or with weight $w_k \in [0,1]$ if i is a k^{th} hexagon ring neighbour in $N_{i,k}$ of a BSS. $\bar{H} \subseteq H$ is the subset of hexagons that already contain an existing BSS. The aim of the optimisation is to maximise the sum of covered demand scores, while limiting the total coverage of a region to a maximum value of $M > 0$. As described in the study [13], the model allows arbitrary values of M but we set the value of $M=1$ here to prevent higher density of BSSs near regions with high demand scores (c_i).

The optimisation problem was setup as shown in Eq. (4) – (9).

$$\max \sum_{i \in H} c_i x_i \quad (4)$$

Subject to:

$$\sum_{i \in H \setminus \bar{H}} y_i \leq R \quad (5)$$

$$y_i = 1 \quad \forall i \in \bar{H} \quad (6)$$

$$x_i \leq w_0 y_i + \sum_{k=1}^n \sum_{j \in N_{i,k}} w_k y_j \quad \forall i \in H \quad (7)$$

$$0 \leq x_i \leq M \quad \forall i \in H \quad (8)$$

$$y_i \in \{0,1\} \quad \forall i \in H \quad (9)$$

The objective function is defined in Eq. (4) and aims to maximise the sum of the covered combined demand scores. The constraint defined in Eq. (5) limits the total number of new BSSs to be built by R , a value chosen by the BSS planner. Constraint (6) sets all existing regions with a BSS to a value of 1. The coverage constraint in Eq. (7) ensures that a region i is covered with corresponding weightings if at least i or one of its k rings of neighbours $N_{i,k}$ is selected for placing a BSS. The feasibility ranges for the variables are defined in Eq. (8) and (9).

To implement the model, a hexagonal hierarchical geospatial indexing system developed by Uber, called H3 [14], was used to partition the analysis area into hexagons with unique index values. The optimisation was implemented as an MILP problem using PuLP [23], a Linear Programming modeler written in Python.

energy futures lab

An institute of Imperial College London

Contact us:


Imperial.ac.uk/energy-futures-lab
energyfutureslab@imperial.ac.uk

 [energyfutureslab](https://www.facebook.com/energyfutureslab)

 [@EnergyFuturesIC](https://twitter.com/EnergyFuturesIC)

 [energyfutureslab](https://www.instagram.com/energyfutureslab)

 [youtube.com/c/EnergyFuturesLabIC](https://www.youtube.com/c/EnergyFuturesLabIC)

 [linkedin.com/company/imperial-college-london-energy-futures-lab](https://www.linkedin.com/company/imperial-college-london-energy-futures-lab)